1   **A multi-tracer approach to constraining artesian groundwater discharge into an**

2   **alluvial aquifer**

3

4

5   **Authors:** Charlotte P. Iverach[1,2,3], Dioni I. Cendón[1,2,3], Karina T. Meredith[3], Klaus M.

6   Wilcken[3], Stuart I. Hankin[3], Martin S. Andersen[1,4], Bryce F.J. Kelly[1,2,*]

7

8

9   [1]Connected Waters Initiative Research Centre, UNSW Sydney, NSW, 2052, Australia

10   [2]School of Biological, Earth and Environmental Sciences, UNSW Sydney, NSW, 2052,

11   Australia.

12   [3]Australian Nuclear Science and Technology Organisation, New Illawarra Rd, Lucas

13   Heights, NSW, 2234, Australia.

14   [4]School of Civil and Environmental Engineering, UNSW Sydney, NSW, 2052, Australia.

15

16

17   *Corresponding author: bryce.kelly@unsw.edu.au

18

19

20

21

22

23

24

Understanding pathways of recharge to alluvial aquifers is important for maintaining sustainable access to groundwater resources. Water balance modelling is often used to proportion recharge components and guide sustainable groundwater allocations. However, it is not common practice to use hydrochemical evidence to inform and constrain these models. Here we compare geochemical versus water balance model estimates of artesian discharge into an alluvial aquifer, and demonstrate why multi-tracer geochemical analyses should be used as a critical component of water budget assessments. We selected a site in Australia where the Great Artesian Basin (GAB), the largest artesian basin in the world, discharges into the Lower Namoi Alluvium (LNA), an extensively modelled aquifer, to convey the utility of our approach. Water stable isotopes (δ^{18}O and δ^{2}H) and the concentrations of Na^+ and HCO_3^- suggest a continuum of mixing in the alluvial aquifer between the GAB (artesian component) and surface recharge, whilst isotopic tracers (^{3}H, ^{14}C and ^{36}Cl) indicate that the alluvial groundwater is a mixture of groundwaters with residence times of < 70 years and groundwater that is potentially hundreds of thousands of years old, which is consistent with that of the GAB. In addition, Cl^- concentrations provide a means to calculate a percentage estimate of the artesian contribution to the alluvial groundwater. In some locations, an artesian contribution of up to 70% is evident from the geochemical analyses, a finding that contrasts previous regional scale water balance modelling estimates that attributed 22% of all inflow for the corresponding zone within the LNA to GAB discharge. Our results show that hydrochemical investigations need to be undertaken as part of developing the conceptual framework of a catchment water balance model, as they can improve our understanding of recharge pathways and better constrain artesian discharge to an alluvial aquifer.

1 Introduction

Groundwater type mixing in an alluvial aquifer can occur between recently recharged groundwater (via infiltration from the land surface) and groundwater discharging into the alluvium from surrounding geological formations and artesian groundwater resources (Costelloe et al. 2012; Schilling et al. 2016; Rawling & Newton 2016; Salameh et al. 2017). Insufficient spatial and temporal data resolution, as well as heterogeneity in hydrogeological properties can result in considerable uncertainty when proportioning contributions from various sources in groundwater with mixed origins (Anderson & Woessner 1992; Beven 2009; Gardner et al. 2012). Additional uncertainties confounding source attribution include change in the magnitude of groundwater gradients and directions over time due to ongoing groundwater abstraction (for irrigation, stock and domestic water supplies), and the impact that this and flood frequency may have on the extent of artesian discharge and groundwater mixing. These complexities make it challenging to accurately proportion contributions from various sources to an alluvial aquifer and to guide water allocations.

Water balance modelling of alluvial aquifers is commonly used to quantify and proportion recharge inputs from river leakage, floodwaters, areal (diffuse recharge) and discharge from artesian sources (Anderson & Woessner 1992; Middlemis et al. 2000; Zhang et al. 2002; Dawes et al. 2004; Barnett et al. 2012; Giambastiani et al. 2012; Hocking & Kelly 2016). Historically, hydrochemical analyses are not often used to constrain catchment scale water balance modelling (Reilly and Harbaugh 2004; Barnett et al. 2012), despite Scanlon et al. (2004) highlighting the need to use multiple techniques (including hydrochemical insights) to increase the reliability of recharge and discharge estimates. Geochemical data can improve our understanding of groundwater mixing processes because of the potential to trace pathways of groundwater movement and water-rock interactions, whilst also providing insights on the impacts of past groundwater extractions (Edmunds 2009; Martinez et al.

74 2017). Therefore, the integration of geochemical evidence to constrain aquifer water balance

75 models provides a more rigorous approach for proportioning input sources for groundwater

76 that has mixed origins (Raiber et al. 2015; Currell et al. 2017).

77 Radioactive isotopic tracers that provide insights into groundwater residence times can

78 constrain mechanisms of recharge and discharge, and detect groundwater mixing. Isotopes of

79 dissolved species can be useful for elucidating groundwater mixing provided the different

80 sources of groundwater have distinctly different and consistent isotopic signatures. However,

81 each tracer has a different half-life and both physical and chemical processes and calculation

82 assumptions can affect the interpretation of groundwater residence times (Jasechko 2016).

83 Therefore, multiple tracers are useful for covering the relevant time scales and uncertainties

84 associated with the large range of groundwater residence times. Tritium (^{3}H) is an excellent

85 indicator of modern recharge inputs in shallow groundwater (Robertson et al. 1989; Chen et

86 al. 2006; Duvert et al. 2016), and provides valuable information on processes active in the

87 past ~ 70 years. Carbon-14 (^{14}C) is used to understand processes active from modern to ~ 30

88 ka (Clark & Fritz 1997; Cartwright et al. 2010; Cendón et al. 2014) and chlorine-36 (^{36}Cl),

89 whilst applicable in modern groundwater (Tosaki et al. 2007), is usually reserved for the

90 identification of much older groundwater (100 ka to 1 Ma). One of the challenges of using

91 ^{36}Cl is that, in certain cases, nucleogenic production of ^{36}Cl can be significant and/or varying

92 Cl concentrations can complicate groundwater residence time interpretations. Additionally,

93 the interpretation of ^{36}Cl can be affected by the input function, as ^{36}Cl values from rainfall

94 vary temporally. This means that the input function for rainfall from any time in the past may

95 be different from current conditions (Phillips 2000). However, in regions with low and fairly

96 consistent Cl concentrations (such as in our study area), ^{36}Cl values can provide solid

97 indications of old groundwater residence times (Mahara et al. 2007).

98   These isotopes can also be used for tracer mixing calculations independent of residence

99   time estimations (Bentley et al. 1986; Andrews & Fontes 1993; Love et al. 2000; Moya et al.

100   2016). Therefore, the combination of ^{3}H, ^{14}C, and ^{36}Cl dating techniques can provide

101   hydrochemical process insights that cannot be captured by using only one isotope.

102   Identification of recharge and discharge pathways (particularly from underlying

103   artesian contributions), and proportioning their relative contributions in a groundwater

104   sample can be better constrained by combining traditional geochemical data with multiple

105   dating techniques and other hydrologic analyses (Amiri et al. 2016; Rawling & Newton 2016;

106   Schilling et al. 2016). This is because groundwater geochemical data give insights into long-

107   term patterns of mixing and groundwater flow, whereas other hydrologic data (such as

108   hydraulic head differences) provide insights on seasonal pumping impacts, and current local

109   and catchment-scale groundwater flow paths.

110   Here, we present for the first time a multi-tracer approach to constraining artesian

111   discharge from the Great Artesian Basin (GAB) into the Lower Namoi Alluvium (LNA),

112   north-west New South Wales (NSW), Australia (Figure 1). We use water stable isotopes and

113   major ion data to assess the major recharge and discharge pathways and occurrences of

114   groundwater mixing in the LNA. We also use ^{3}H, ^{14}C and ^{36}Cl to show that artesian discharge

115   from the underlying GAB to the LNA is locally much higher than is currently estimated from

116   water balance models used to guide groundwater allocations in the region (Lower Namoi

117   Groundwater 2008). Our results highlight the need to consider a multi-tracer geochemical

118   approach when assessing artesian contributions to alluvial aquifers and constraining water

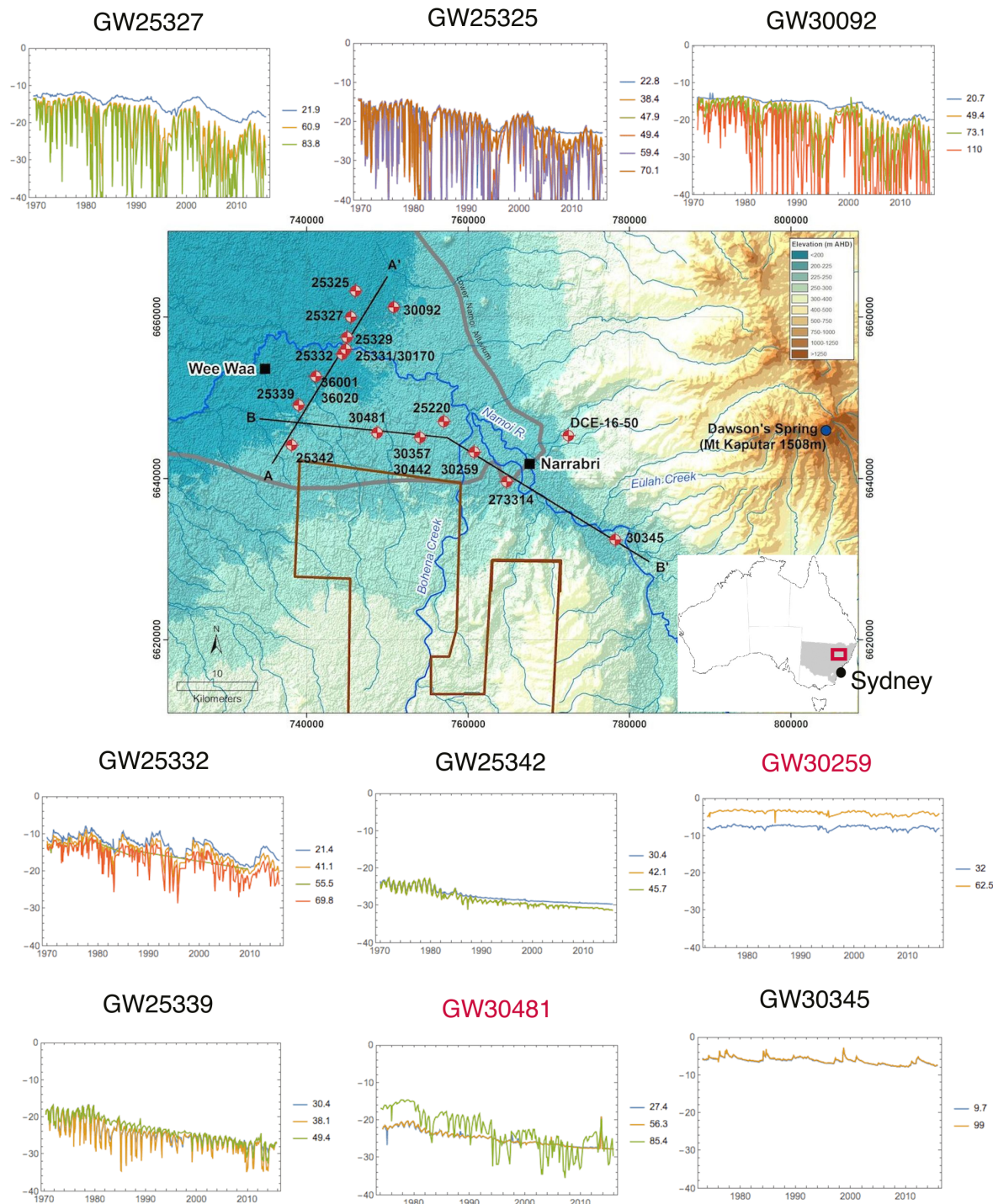119   balance models of alluvial systems globally.

Figure 1. Map of the study area and sample locations, along with the location of the study area in Australia. Accompanying hydrographs show the groundwater level response in different piezometers throughout the study area (groundwater level data sourced from BOM 2017). The different colours in the hydrographs represent the different monitoring bores in the nested set. The bottom of the slotted

125 interval for each bore is shown in the key. The x-axis in each hydrograph is the year (1970-2010) and

126 the y-axis is depth (between 0 and 40 m below ground surface (bgs)). The two locations with red text

127 highlight areas where the hydrograph heads show clear GAB contribution, with the deeper piezometer

128 showing a higher head than the shallow one. The remaining locations show no apparent GAB

129 contribution to the LNA based on the hydrograph data.

130

131 **2   Study Area**

132 The lower Namoi River catchment is located in the north-west of NSW, Australia (Figure 1).

133 Groundwater resources in the LNA are the most intensively developed in NSW (DPI Water

134 2017). For this reason, there is concern regarding groundwater exploitation and threat to the

135 long-term sustainability of the system (Lower Namoi Groundwater 2008; DPI Water 2017).

136 Groundwater abstraction from the LNA supports a multibillion-dollar agricultural sector

137 (focused around cotton growing established in the 1960s), supplying around 50% of water for

138 irrigation in the region (Powell et al. 2011). Peak extraction of approximately 170 x 10^6 m^3

139 occurred over the 1994/1995 growing season (Smithson 2009). Consistently declining

140 groundwater levels and concern regarding the long-term sustainability of groundwater

141 abstraction led to the implementation of a Water Sharing Plan in 2006, which systematically

142 reduced groundwater allocations to the irrigation sector over a ten-year period. The present

143 allocation is 86 x 10^6 m^3 /year (Lower Namoi Groundwater 2008).

144

145 **2.1   Hydrogeological setting**

146 The lower Namoi River catchment lies within the Murray-Darling Basin, overlying the

147 Coonamble Embayment, which is in the south-east portion of the GAB (Radke et al. 2000).

148 The southernmost portion of the LNA is underlain by Triassic formations, while northwest of

149 monitoring bore 30345 the LNA is underlain by Jurassic formations (Figure 2). Within the

150 region of study, the oldest outcropping bedrock formation is the early Triassic Digby

151   Formation (lithic and quartz conglomerates, sandstones and minor finer grained sediments)

152   (Tadros 1993). The Digby Formation outcrops in the south-east of the area and the Namoi

153   River abuts the formation just south of B' on Figure 2. The Digby Formation is overlain by

154   the Triassic Napperby Formation (thinly bedded claystone, siltstones and sandstone). This

155   formation occurs at a depth of 106 m, just below the base of monitoring bore 30345 (NSW

156   Pinneena Groundwater Database, driller logs).In outcrops to the east of the study area, the

157   Napperby Formation is overlain by the late Triassic Deriah Formation (green lithic sandstone

158   rich in volcanic fragments and mud clasts) (Tadros 1993). The boundary between the Triassic

159   and Jurassic lies west of monitoring bore 30345. The Jurassic formations important to this

160   study are the Purlawaugh Formation (carbonaceous claystone, siltstone, sandstone and

161   subordinate coal), Pilliga Sandstone (medium to coarse quartzose sandstone) and the Orallo

162   Formation (clayey to quartzose sandstone, subordinate siltstone and conglomerate) (Tadros

163   1993). The Pilliga Sandstone forms the bedrock below monitoring bores 25325 to 25342, and

164   in the Namoi region is the primary aquifer of the GAB.
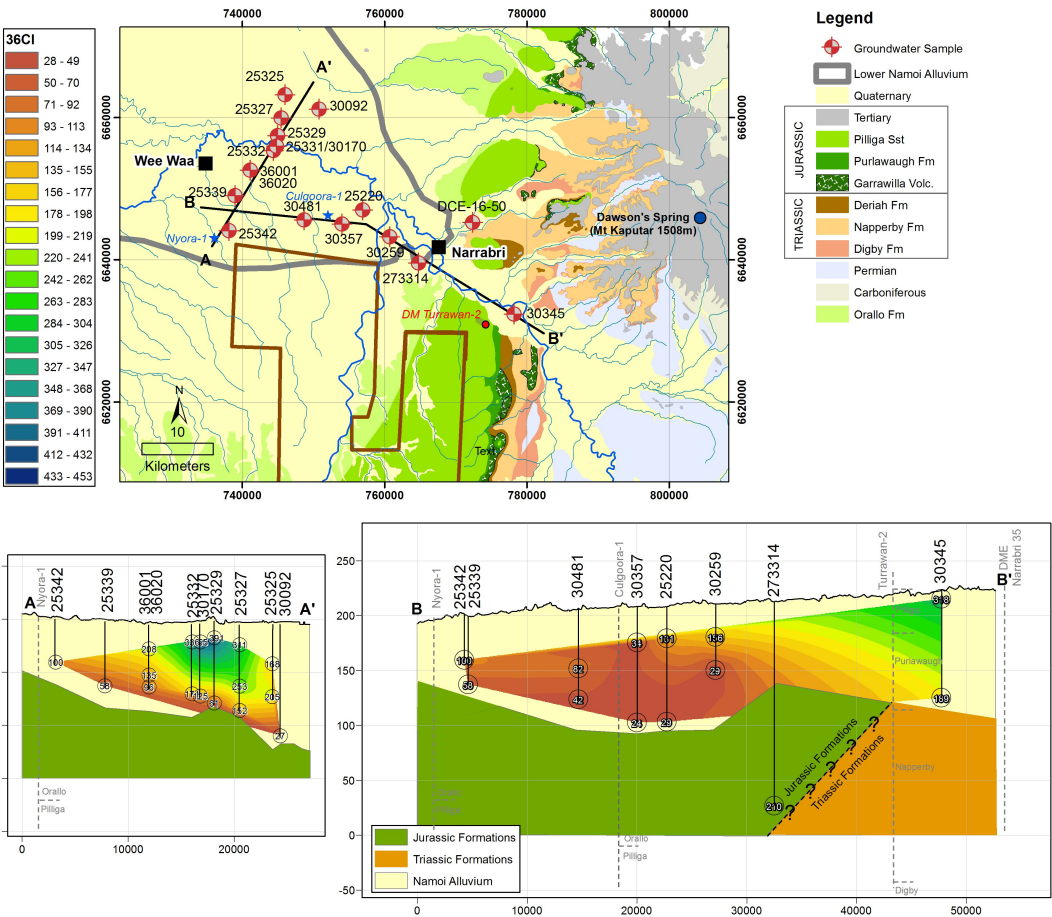
166

Figure 2. A geological map of the study area and two cross sections through the study area, showing the location and depth of the samples in the alluvium and their proximity to formations of the GAB. Contacts obtained from gas wells Nyora-1, Culgoora-1 and Turrawan-2, coinciding with our cross sections, are added. Their locations are displayed on the map. The general direction of groundwater flow is from SE to NW, aligning with the B-B' line on the map. The chlorine-36 data interpolated using the 'natural neighbours' algorithm is shown in each cross section.

173

From the late Cretaceous to the mid Miocene, a palaeovalley was carved through the basement rocks (Kelly et al. 2014). Then from the mid Miocene until present, the palaeovalley was filled with reworked alluvial sediments. Groundwater abstraction in the study area is mostly from these alluvial sediments. Fluvial and aeolian interbedded clays, silts, sands and

178   gravels form the up to ~ 140 m thick alluvial sequence of the Lower Namoi Catchment

179   (Williams et al. 1989). Traditionally, three main non-formally defined aquifers/formations have

180   been used to describe the LNA. The semi-confined Cubbaroo Formation overlies the bedrock in

181   the northern palaeochannel (which passes beneath monitoring bores 25325 and 30092). This

182   formation is up to 60 m thick. The Cubbaroo Formation is overlain by the semi-confined

183   Gunnedah Formation, which is up to 80 m thick, and is conformably overlain by the unconfined

184   Narrabri Formation, which is 10 to 40 m thick (Williams et al. 1989). However, recent studies

185   in the Namoi Catchment suggest that the rigid subdivision in to the Narrabri, Gunnedah, and

186   Cubbaroo formations cannot easily explain the continuum in chemical evolution observed

187   (discussed further below) and that the valley filling sequence is better characterised as a

188   distributive fluvial system (Kelly et al. 2014, Acworth et al. 2015).

189   Groundwater drains from the Upper Namoi into the LNA via a bedrock constriction north

190   of Narrabri and generally flows from east to west within the LNA (Barrett 2012). Hydraulic

191   conductivity in the alluvial aquifer is highly variable (0.008-31 m/day) due to the presence of

192   variable sand and clay (Golder Associates 2010). However, hydraulic conductivity generally

193   increases with depth.

194

195   **2.2   Current understanding of recharge and discharge processes in the Lower Namoi**

196   **Alluvium**

197   There have been numerous catchment water balance models and hydrochemical

198   investigations in the study area because of the local and national economic importance of the

199   LNA. However, the hydrochemistry of the groundwater in the region has not been used in

200   conjunction with water balance modelling prior to this study (Merrick 2000; CSIRO 2007;

201   Kelly et al. 2007).

202

203   *2.2.1   Water balance modelling of recharge*

204   To guide groundwater allocations from the LNA, a series of water budget models were

205   developed using MODFLOW (Merrick 2000; summarised in Kelly et al. 2007). These

206   models were driven by climatic, rainfall, flood and streamflow data and calibrated to

207   groundwater head data. There are multiple plausible solutions for all water balance models

208   and the solution presented is often constrained by several factors. These constraining factors

209   include geological insights; the modeller's experience and biases (such as, for example, the

210   way diffuse recharge is modelled either as a percentage of rainfall (Merrick 2000; CSIRO

211   2007) or as a complex evapotranspiration function (Giambastiani et al. 2012)); verification

212   measures and pragmatic goals. One MODFLOW derived water balance model proportioned

213   the recharge for the water budget period 1980-1994 as following: flood and diffuse rain

214   recharge 24.1 x 10^5 m^3 /year, stream recharge 33.7 x 10^5 m^3 /year, up gradient alluvial inflow

215   3.06 x 10^5 m^3 /year, and artesian (GAB) recharge 9.5 x 10^5 m^3 /year. In that model, artesian

216   recharge was inferred to occur in the eastern portion of the model (between Narrabri and Wee

217   Waa), which overlaps with this study area (Figure 1). The zone between Narrabri and Wee

218   Waa accounted for 42.7 x 10^5 m^3 /year of the total recharge to the LNA. Thus, according to

219   the model, GAB discharge into the LNA in this area equated to 22%. When the LNA

220   MODFLOW model was calibrated there was no consideration given to using hydrochemical

221   data to constrain the calibration (Merrick 2000; CSIRO 2007; Kelly et al. 2007).

222

223   *2.2.2   Hydrochemical estimates of recharge*

224   The first isotopic investigation in the area was conducted from 1968 to 1975 and partially

225   published by Calf (1978). The author used ^{14}C and ^{3}H to assess recharge pathways to the

226   LNA and found evidence for river recharge in the upper aquifer, and that modern

227   groundwater penetrated the deeper parts of the LNA. Calf (1978) also found evidence for

228 'leakage' of groundwater from the GAB up into the deeper LNA, however volumetric

229 estimates were not provided.

230 McLean (2003) conducted an extensive hydrochemical and isotopic characterisation of

231 both the GAB groundwater and the alluvial groundwater in 1999-2000. This research

232 concluded that mixing of groundwater from the GAB into the lower and middle parts of the

233 LNA is an important process especially in the south of the catchment. This study also did not

234 quantify the amount of mixing occurring between the two groundwater sources.

235 The over-reliance of water balance models used to allocate groundwater resources that

236 have not been constrained by isotopic tracer residence times or hydrochemical results is a

237 common issue globally. This research highlights that hydrochemical investigations improve

238 our conceptual understanding of recharge pathways and that such investigations should be

239 applied to all important groundwater resource assessments to enable sustainable management.

240

241 **3   Materials and methods**

242 **3.1   Groundwater collection**

243 This study comprised two field campaigns, the first one from 28 January 2016 to 8 February

244 2016 (summer) when the aquifer was stressed by pumping for irrigation, and the second from

245 21 June 2016 to 30 June 2016 (winter) in the absence of abstraction for irrigation.

246 In summer, 28 groundwater samples were collected from NSW Department of Primary

247 Industries Water (DPI Water) monitoring bores and a surface water sample from the Namoi

248 River. In winter, 16 groundwater samples were collected from NSW DPI Water monitoring

249 bores and surface water samples from the Namoi River and 2 upstream tributaries (see

250 Supplementary Table 2 for locations). The bores are screened at varying intervals (average

251 length of screened interval: 5.6 m (see Supplementary Table 2 for individual bores)),

252 intersecting the shallow, middle and deep alluvium. Most bores were sampled with either a

253   Grundfos (MP1 sampling pump) or Bennett compress air piston pump, with the pump placed ~

254   1 m above the screen when using the Grundfos pump. Drop-tube extensions were used with the

255   Bennett pump to place the pump intake just above the screen. Some deep monitoring bores

256   were sampled with a portable bladder pump using low-flow methods (Puls & Barcelona, 1996).

257   In these bores the pump was placed approximately 10 m below standing water level, with a

258   drop-tube cut to place the pump intake within the screen. For shallower bores (less than 50 m),

259   a 12 V battery operated pump was used with the pump intake placed ~1 m above the screen.

260   For all sample sites, physico-chemical parameters (pH, DO, EC) were monitored and samples

261   collected once three well volumes had been pumped and/or the physico-chemical parameters

262   stabilised. This was generally achieved within 1 to 3 hours after onset of pumping. Sample

263   collection involved an in-line, 0.45 μm, high-volume filter connected to a high-density

264   polyethylene (HDPE) tube. Total alkalinity concentrations (field alkalinity) were determined in

265   the field by acid titration using a HACH digital titrator and external pH meter control. The Fe^{2+}

266   and HS^- concentrations were determined using a portable colorimeter (HACH DR/890).

267   Samples for anion and water stable isotope (δ^2H and $\delta^{18}O$) analyses were collected in 60

268   mL and 30 mL HDPE bottles, respectively, with no further treatment. Samples for cation

269   analysis were collected in 60 mL HDPE bottles and acidified with ultrapure nitric acid.

270   Samples for ^{14}C and ^3H were collected in 1 L narrow mouth HDPE bottles and 2 L HDPE

271   bottles respectively, and were sealed with tape to avoid potential atmospheric exchange during

272   storage. Samples for ^{36}Cl were collected in 1 L narrow mouth HDPE bottles with no further

273   treatment. Major ion and ^{14}C samples were refrigerated at 4^oC until analysed.

274   We were not able to access any previously sampled GAB bores within the study area.

275   Thus, better constrain GAB groundwater characteristics, we used geochemical data from

276   known GAB bores collected by Radke et al. (2000) and McLean (2003). These data were

277   collected to the northwest of our study area and are used as a range (depending on availability

278   of the original reported data) for the GAB end-member in our discussions (Supplementary

279   Table 1).

280   To help in the description of results, we use shallow (< 30 m), intermediate (30 − 80 m)

281   and deep (> 80 m) as a rough guide to the origin of the groundwater sample. The chosen depth

282   categories are based on clusters and trends in the ^{14}C analyses.

283

284   **3.2   Geochemical analyses**

285   Groundwater samples from both campaigns were analysed at ANSTO by inductively coupled

286   plasma atomic emission spectroscopy (ICP-AES) for cations and ion chromatography (IC) for

287   anions. Samples for δ^2H and δ^{18}O were analysed using Cavity Ring-Down Spectroscopy

288   (CRDS) on a Picarro L2130-*i* analyser. These values are reported as ‰ deviations from the

289   international standard V-SMOW (Vienna Standard Mean Ocean Water) and results have a

290   precision of ± 1‰ for δ^2H and ± 0.15‰ for δ^{18}O.

291   The ^{14}C samples were processed and analysed at ANSTO using methods described in

292   Cendón et al. (2014). The ^{14}C activities were measured by accelerator mass spectrometry

293   (AMS) using the ANSTO 2MV tandetron accelerator, STAR (Fink et al. 2004). The ^{14}C results

294   were reported as percent modern carbon (pmc) following groundwater ^{14}C reporting criteria

295   (Mook & van der Plicht 1999; Plummer & Glynn 2013) with an average 1σ error of 0.21 pmc.

296   The ^{3}H samples were analysed at ANSTO. Water samples were distilled and

297   electrolytically enriched prior to analysis by liquid scintillation. The ^{3}H concentrations were

298   expressed in tritium units (TU) with a combined standard uncertainty of ± 0.03 TU and

299   quantification limit of 0.04 TU. Tritium was measured by counting beta decay in a liquid

300   scintillation counter (LSC). A 10 mL sample aliquot was mixed with the scintillation cocktail

301   that releases a photon when struck by a beta particle. Photomultiplier tubes in the counter

302   convert the photons to electrical pulses that are counted over 51 cycles for 20 minutes.

303   The ^{36}Cl/Cl and ^{36}Cl/^{37}Cl ratios were measured by AMS using the ANSTO 6MV SIRIUS

304   Tandem Accelerator (Wilcken et al. 2017). Samples were processed in batches of 10, with

305   each batch containing 1 chemistry blank. The amount of sample used was selected to yield ~

306   5 mg of Cl for analysis without carrier addition. Chloride was recovered from the sample

307   solutions by precipitation of AgCl from hot solution (Stone et al. 1996). This AgCl was re-

308   dissolved in aqueous NH_3 (20-22 wt %, IQ grade, Seastar) to remove sulfur compounds of Ag.

309   Owing to isobaric interference of ^{36}S with ^{36}Cl in the AMS measurements, a saturated

310    $Ba(NO_3)_2$ solution (99.999% trace metal basis) was used to precipitate sulfur as $BaSO_4$. At

311   least 72 h were allowed for $BaSO_4$ to settle from a cold solution (4℃) in the dark before

312   removal of the supernatant by pipetting and filtration (0.22 Millex GS). Pure AgCl was re-

313   precipitated by acidifying the $Ag(NH_3)_2$-Cl solution with 5M nitric acid (IQ Seastar, sub-

314   boiled). Finally, AgCl was recovered, washed twice and dried. It was then pressed into high-

315   purity AgBr (99% trace metal basis, Aldrich) in 6 mm diameter Cu-target holders. AgBr has a

316   much lower sulfur content than Cu. The stable Cl isotopes ^{35}Cl and ^{37}Cl were measured with

317   Faraday cups and ^{36}Cl events were counted with a multi-anode gas ionisation chamber. Gas

318   (Ar) stripping (for good brightness/low ion straggling) the ions to 5+ charge state in the

319   accelerator terminal suffices for effective ^{36}S interference separation in the ionisation chamber

320   combined with sample-efficient and rapid analysis. Purdue PRIMELab Z93-0005 (nominally

321   1.20×10^{-12} ^{36}Cl/Cl) was used for normalisation with a secondary standard (nominally 5.0×10^{-13}

322   ^{36}Cl/Cl (Sharma et al. 1990)) used for monitoring. Background subtraction was done with a

323   linear dependence between ^{36}Cl-rate and interfering ^{36}S-rate. This dependency is established by

324   combining all the blank and test sample measurements and applied to the unknown samples

325   during offline data analysis. This correction factor was typically less than analytical uncertainty

326   of 3-4% bar one sample that had a correction factor of 12% with an analytical uncertainty of

327   6%.

328

3.3   Geochemical calculations

Calculations necessary to assess electrical neutrality, dissolved element speciation and saturation indices for common mineral phases were undertaken using the PHREEQC Interactive program (3.3.8) (Parkhurst & Appelo 1999) and the incorporated WATEQ4F thermodynamic database (Ball & Nordstrom 1991). The cation and anion analyses were assessed for accuracy by evaluating the charge balance error percentage (CBE%). All samples fell within the acceptable ± 5% range, except for samples 25327-1 (-7.8 %) and 36001-1 (-5.8 %). The inverse geochemical modelling code NEPATH XL (Plummer et al. 1994; Parkhurst & Charlton 2008) has been used to calculate the mixing ratio between two end-members, using their Cl concentrations. The choice of end-members will influence calculated proportions, however, end-members were selected to provide conservative approximations.

Despite limitations, ^{36}Cl residence times for selected low ^{36}Cl/Cl samples were calculated from the equations of Bentley et al. (1986). This allows a direct comparison, under similar assumptions, with other estimates obtained from GAB groundwater elsewhere (Bentley et al. 1986; Radke et al. 2000; Love et al. 2000; Moya et al. 2016) and within the Coonamble Embayment (Radke et al. 2000; Mahara et al. 2007). These calculations assume a piston flow setting with no other sources or sinks besides recharge and natural decay (eqn. 1):

$$t = \frac{-1}{\lambda_{36}} \ln \frac{R - R_{se}}{R_0 - R_{se}} \tag{1}$$

where R = ^{36}Cl/Cl ratio measured in the sample, R_0 = the initial ^{36}Cl/Cl ratio (meteoric water), R_{se} = the ^{36}Cl/Cl ratio under secular equilibrium (in this case the ^{36}Cl/Cl ratio from the Pilliga Sandstone), and λ_{36} is the decay constant (2.303 x 10^{-6}). We used a R_0 value of 160 (x10^{-15}), which was an average of 10 samples compiled from studies in the Coonamble Embayment and reported in Radke et al. (2000). For R_{se} a value of 5.7 (x10^{-15}) was used, which is appropriate for aquifers dominated by sandstone (this secular equilibrium value can

353 vary according to the dominant lithology). This R_{se} value has been applied to [36]Cl/Cl

354 calculations elsewhere in the GAB (Moya et al. 2016) and is similar to that calculated from

355 drill-core samples recovered in the GAB by Mahara et al. (2009).

356

357 **4   Results**

358 **4.1   Major ion chemistry**

359 The groundwater of the alluvial aquifer is predominantly Na-HCO$_3$-type water, with

360 concentrations ranging from 0.12 mmol/L to 54.6 mmol/L (average: 6.85 mmol/L; std dev:

361 8.7 mmol/L) for Na$^+$ and 0.29 mmol/L to 24.0 mmol/L (average: 6.43 mmol/L; std dev: 4.8

362 mmol/L) for HCO$_3^-$ (Supplementary Table 2). Generally, the highest concentrations of Na$^+$

363 and HCO$_3^-$ occur in the deeper groundwater and decrease up the vertical groundwater profile

364 (Figure 3a). The concentration of these two ions in the groundwater of the LNA is higher

365 than expected from local rainfall sources and other shallow groundwater alluvial systems in

366 eastern Australia (Martinez et al. 2017). In GAB groundwater, the Na-HCO$_3$ molar ratio is

367 generally 1:1 and the two ions are generally present in higher concentrations than in our

368 alluvial samples (Radke et al. 2000; McLean 2003), which is evident in the position of the

369 regional GAB samples in Figure 3a.

370   Additional ions used in this study are F$^-$, Cl$^-$ and the Cl/Br ratio. The concentration of F$^-$

371 in the groundwater ranges from 0.002 mmol/L to 0.215 mmol/L (average: 0.028 mmol/L; std

372 dev: 0.04 mmol/L). Fluoride concentrations generally increase with depth and accumulate in

373 solution as all groundwater samples are below saturation with respect to fluorite (Figure 3b).

374 Concentrations of Cl$^-$ in the alluvial groundwater range from 0.063 mmol/L to 26.73 mmol/L

375 (average: 1.67 mmol/L; std dev: 3.7 mmol/L). Unlike the other major ions, Cl$^-$ concentrations

376 through the vertical groundwater profile are relatively stable (Figure 3c). The relationship

377 between Cl$^-$ and the Cl/Br ratio shows that groundwater composition clusters from values

378   below the seawater ratio to values close to seawater. The Cl/Br ratios are similar to ranges

379   found in other alluvial groundwater systems but slightly lower than ratios observed in other

380   GAB samples for Australian locations (Herczeg et al., 1991; Cendón et al., 2010; Cartwright

381   et al., 2010). Additionally, the Cl/Br ratios in shallow samples connected to the river are

382   consistent with expected ratios in rainfall (Short et al. 2017). The regional GAB samples

383   (Radke et al. 2000) show a Cl/Br ratio more similar to seawater, with our samples from the

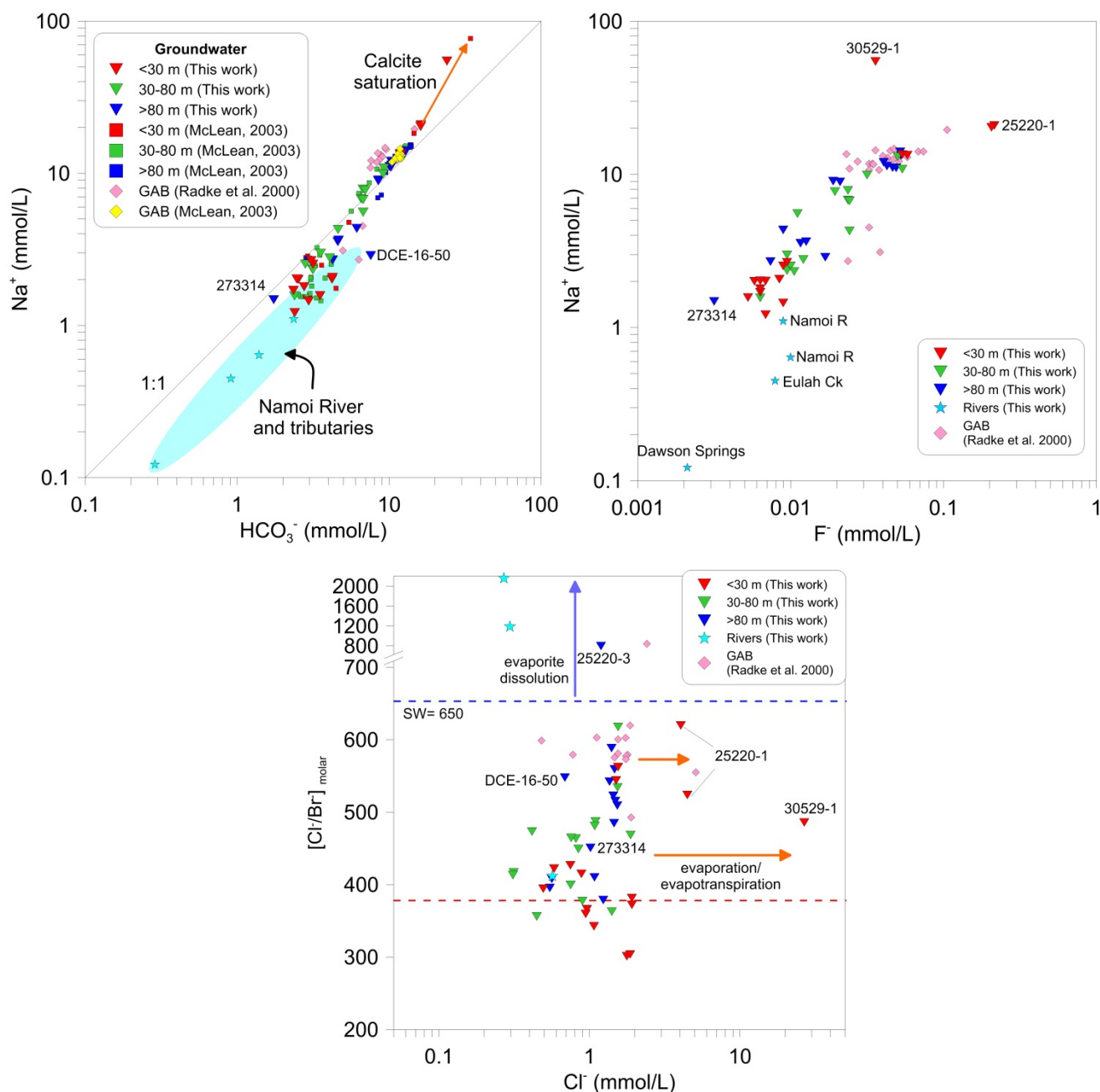384   LNA lying on a mixing trend between the two end-members (Figure 3c).

385

Figure 3. a) Na$^+$ vs HCO$_3^-$ showing the mixing trend that the alluvial samples form between the Namoi River and samples from the GAB (Radke et al. 2000; McLean 2003). The orange calcite saturation line indicates samples that are more enriched due to separate evapotranspiration and calcite precipitation. The shaded blue ellipse represents all river chemistry data available for the Namoi River and tributaries (this work (n=4), McLean 2003 (n=4), Mawhinney 2011 (n=79)); b) Na$^+$ vs F$^-$ and c) Cl$^-$/Br$^-$ vs Cl$^-$, highlighting the mixing trend between the surface recharge and the GAB that we observe in other geochemical indicators. The red dotted line represents the Cl$^-$/Br$^-$ ratio for rainfall and the blue dotted line is the seawater ratio.

19

395   We identified one major outlier in the hydrochemical results, which was sample

396   273314. This sample is from 207 m bgs and the bore screen is classified as being in the GAB.

397   However, the geochemical parameters for this deep GAB sample have a signature more

398   similar to river water than what would be expected in the GAB 207 m bgs. The concentration

399   of Na^+, HCO_3^-, Cl^-, F^- and the Cl/Br ratio in this sample plot closer to the river and shallow

400   groundwater than the deeper groundwater system (Figure 3). Potential reasons for this are

401   explored in detail below.

402

403   **4.2   Stable water isotopes (δ^2H and δ^{18}O)**

404   The stable water isotopic values for this study range from -0.76‰ to 8.4‰ for δ^{18}O and -

405   7.5‰ to -54.9‰ for δ^2H. Most groundwater samples cluster together at around -6‰ and -

406   40‰ (δ^{18}O and δ^2H) and lie on the global meteoric water line (GMWL), to the right of the

407   nearest available local meteoric water lines (LMWL) (Macquarie Marshes and Gunnedah)

408   (Figure 4; Supplementary Table 3). A group of mostly shallow samples collected from

409   piezometers close to river channels define a trend to the right of the GMWL with a slope of

410   5.96, which is consistent with evaporation (Cendón et al. 2014). Our results are similar,

411   including the shallow groundwater evaporative trend, to those recorded by McLean (2003).

412   Water stable isotopic compositions for regional GAB samples range from -6.58‰ to -6.24‰

413   for δ^{18}O and -43.1‰ to -38.8‰ for δ^2H (McLean 2003) (Figure 4).
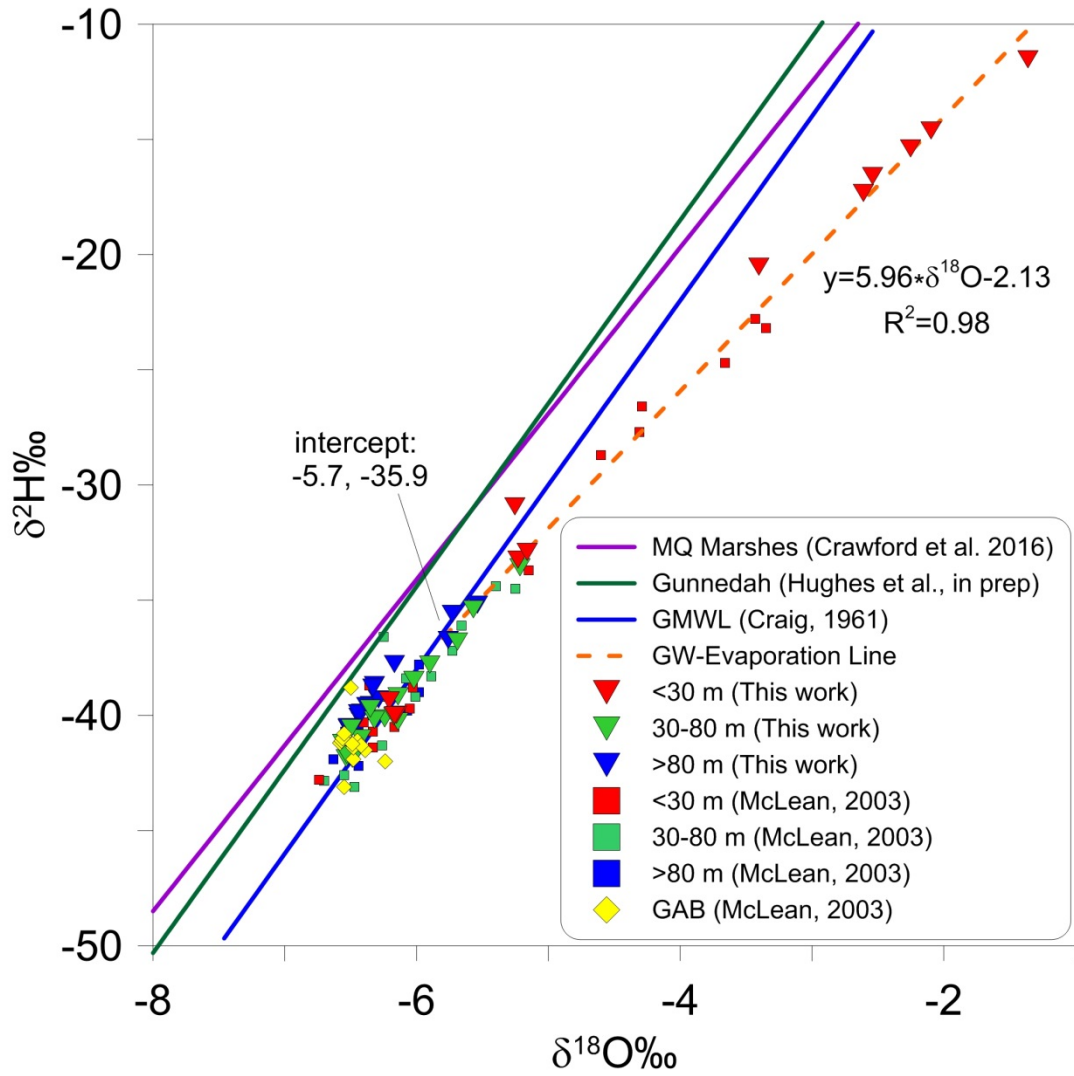
414

Figure 4. Water stable isotopes in the LNA, showing the two separate mechanisms of recharge; surface water recharge plotting along an evaporation trend line and potential inflow from the GAB clustered with regional samples from the GAB (McLean 2003).

4.3   Isotopic tracers (^{3}H, ^{14}C and ^{36}Cl)

Tritium activities vary throughout the study area, ranging from below the quantification limit (< 0.04 TU) to 2.36 TU (average: 0.42 TU). Tritium activities generally decrease with depth and distance from the river channel (Figure 5) (all data in Supplementary Table 3). The highest ^{3}H activities of 2.31 TU and 2.36 TU are from a sample 40 m from the river and the

425   Namoi River itself, respectively. These are very similar to modern rainfall in Australia (~ 2-3

426   TU (Tadros et al. 2014)), which suggests modern recharge near the river channels However,

427   ^{3}H > 0.04 TU was measured at depth (down to 207 m bgs). The ^{3}H activities we measured at

428   depth are significant for Australian groundwater, as the peak of the bomb pulse in Australia

429   was only around 60 TU compared to locations in the northern hemisphere. This is primarily

430   because most thermonuclear testing was undertaken in the northern hemisphere far from

431   Australia and mixing is limited between the atmospheric convection cells in the northern and

432   southern hemispheres. Therefore, ^{3}H in Australian rainfall has been at natural background

433   concentrations for some time (Tadros et al. 2014).
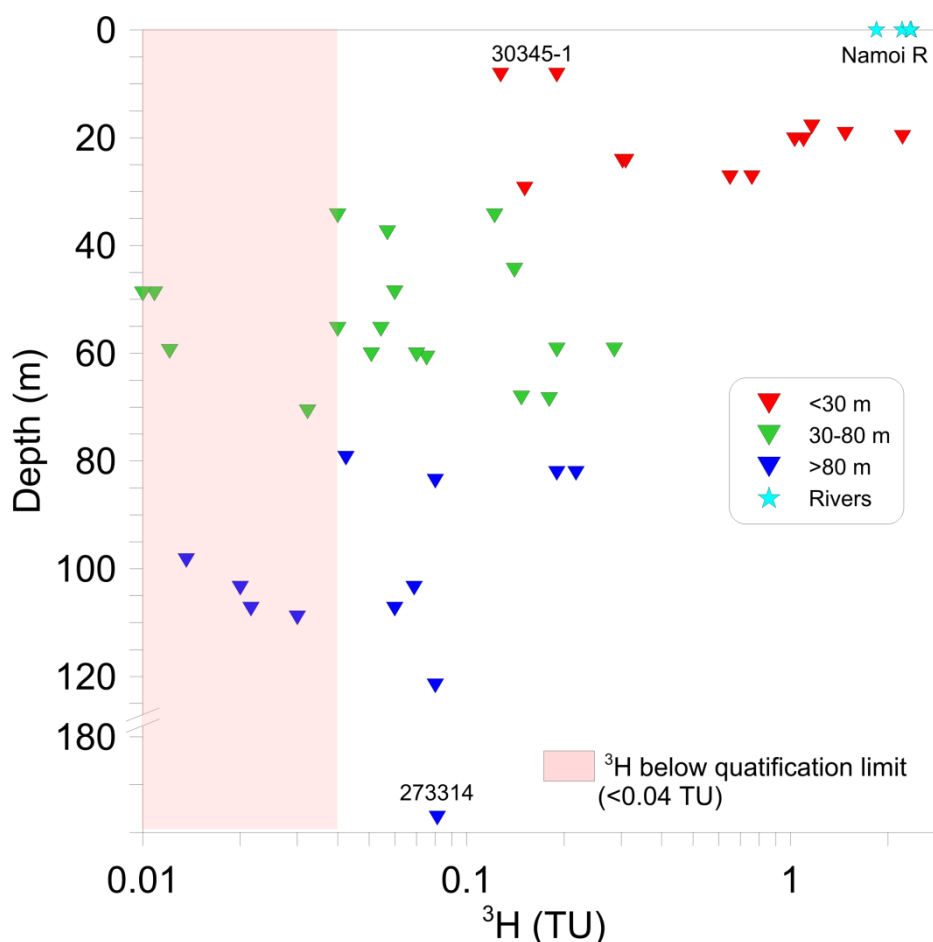
434   **Figure 5.** Plot of depth vs ^{3}H, highlighting the ^{3}H activity throughout the vertical groundwater profile.

435   Samples that fall within the pink zone on the left are below the quantification limit (< 0.04 TU). These

436   data are not included in our interpretation of how ^{3}H changes with depth. They are presented to

437   convey the relative proportions of interpretable versus non-interpretable data.

438   The ^{14}C content in the groundwater ranged from 0.2 pmc to 107.6 pmc (average: 54.0

439   pmc). Generally, groundwater samples shallower than 30 m had a high ^{14}C content (> 90

440   pmc), which decreased with depth. There were 9 samples with a ^{14}C content below 1 pmc,

441   indicating old groundwater (> 30 ka), with total depths ranging from 35 m bgs to 207 m bgs.

442   Our ^{36}Cl results for the alluvial groundwater ranged from 24.06 ($\times 10^{-15}$) to 455.35 ($\times 10^{-15}$)

443   ^{15}) (average: 169.4 ($\times 10^{-15}$) (shown in the interpolation in Figure 2). It has been found that

444   groundwater in the GAB recharge zone closest to the study area has a $^{36}Cl/Cl$ ratio up to ~

445   200 ($\times 10^{-15}$) (Radke et al. 2000) with recharge values applied in calculations elsewhere in the

446   GAB of 110 ($\times 10^{-15}$) (Moya et al. 2016). Water from the Namoi River has a $^{36}Cl/Cl$ ratio of ~

447   420 ($\times 10^{-15}$) (Supplementary Table 4).

448

449   **5   Discussion**

450   **5.1   Identification of recharge and mixing between the GAB and the LNA**

451   The $\delta^{18}O$ and $\delta^{2}H$ isotopic compositions suggest two mechanisms of recharge to the

452   alluvium: artesian discharge and surface water infiltration. The regional GAB samples plot

453   within the alluvial groundwater sample range, suggesting a GAB component in the alluvium.

454   The evaporation line in Figure 4 indicates recharge to the alluvium via surface water

455   infiltration. It also shows a good connection between surface water that has undergone

456   evaporation prior to recharge.

457   Additional evidence for these two mechanisms of recharge is the composition of Na^{+}

458   and HCO_3^{-} in the LNA. Figure 3a shows a mixing line that the alluvial samples follow,

459   plotting between the end-members of the GAB and the Namoi River, suggesting an

460   increasing GAB contribution to the alluvial groundwater with depth. This also implies that a

461 continuum of mixing exists between the shallow and deep groundwater within the LNA. The

462 shallow samples (25220-1 and 30259-1) that are more Na^+ enriched compared to samples

463 from the GAB have undergone separate evapotranspiration processes and hence have a

464 concurrent increase in Cl^-. Assuming that Cl^- is behaving conservatively (Appelo & Postma

465 2005) we surmise that increases in dissolved major ion concentrations concomitant with

466 increases in Cl^- in the shallow groundwater are likely to be a result of evapoconcentration.

467   Further hydrochemical evidence for these recharge mechanisms is the covariation of

468 Na^+ and F^-, both interpreted as primarily derived from groundwater interaction with silicate

469 minerals in this region (Airey et al. 1978; Herczeg et al. 1991; McLean 2003) (Figure 3b).

470 Our alluvial samples fall on the mixing line between samples from the river and nearby

471 tributaries and regional samples from the GAB (Radke et al. 2000), in a similar way to the

472 $Na-HCO_3$ trend that we observe in Figure 3a. The Cl/Br ratios in the groundwater also

473 support the mixing interpretation provided by the Na^+ and HCO_3^- concentrations, contrary to

474 the possibility of water rock interactions along the alluvium flowpath (Figure 3c).

475 Furthermore, the relationship between ^{36}Cl and Na^+ provides additional evidence of mixing in

476 the groundwater (Supplementary Figure 1).

477   Figure 3 also highlights the deep outlying sample (273314), which was 207 m bgs in

478 total depth, yet plots with the shallow alluvial and river samples. Figure 2 shows that this

479 sample is situated just above the Napperby Formation. We hypothesise that this sample

480 originated from surface recharge from the Namoi River (which is in contact with the

481 underlying Digby Formation to the south of the study area), with negligible input from the

482 more $Na-HCO_3$-rich groundwater in the Pilliga Sandstone, where the sample is from. Sample

483 30345-2 (Supplementary Tables 2 and 3), which is situated in the lower part of the LNA in

484 proximity to the alluvial contact with the Napperby Formation (Figure 2) has a similar

485 geochemistry. These results suggest the connection between deeper Triassic formations

486 beneath the GAB and the Namoi River, which must be an important consideration in future

487 water balance models of the catchment.

488

489 *5.1.1 Mixing between groundwaters of varying residence times*

490 Major ion and water stable isotope data suggest two primary mechanisms of recharge to

491 the LNA and show that mixing is occurring within the alluvium. ^{3}H activity and ^{14}C content

492 in the alluvial groundwater to quantify the potential residence times of the groundwater

493 sources that are mixing within the alluvium. Tritium activities > 0.04 TU at depth (down to

494 207 m bgs) indicates the extent of recharge from episodic flooding. Measuring ^{3}H > 0.04 TU

495 at these depths also shows that surface recharge reaches the deeper LNA relatively quickly (<

496 70 years). Tritium data from the 1970's collected from bores that were included in our

497 sampling campaign (25329 and 25332) (Calf 1978) suggest that ^{3}H was already present in the

498 deeper parts of the alluvial aquifer (> 70 m bgs) prior to a major flood in 1971, with activities

499 ranging from 7.9 TU to 11.2 TU. This indicates good connectivity to and recharge from the

500 surface. Additionally, measurements of ^{3}H in these bores post-flooding (16.6 to 20.7 TU)

501 indicate that substantial recharge from the surface took place during this flood. This

502 highlights the importance of surface water recharge to the LNA. The activities of ^{3}H > 0.04

503 TU throughout the vertical profile of the LNA (Figure 5) are inconsistent with the low ^{14}C

504 contents in the groundwater. The presence of measurable ^{3}H but negligible ^{14}C (close to 0

505 pmc) suggests that mixing is occurring between groundwater that is associated with modern

506 recharge processes in the alluvium and groundwater that, as indicated by the ^{14}C content, is

507 presumably much older. This older groundwater may be derived from artesian inflow. Figure

508 6 shows ^{3}H activities > 0.04 TU in samples with ^{14}C content of almost 0 pmc, suggesting that

509 groundwater with a very low ^{14}C content is mixing with groundwater with a high ^{3}H activity.

510 Even though there is evidence of ^{14}C dilution in localised areas, we also observe mixing

511 between groundwaters of widely different ^{14}C and ^{3}H values in the gradient of the samples in

512 Figure 6 (emphasised with a dotted blue line). This gradient would be steeper if there were

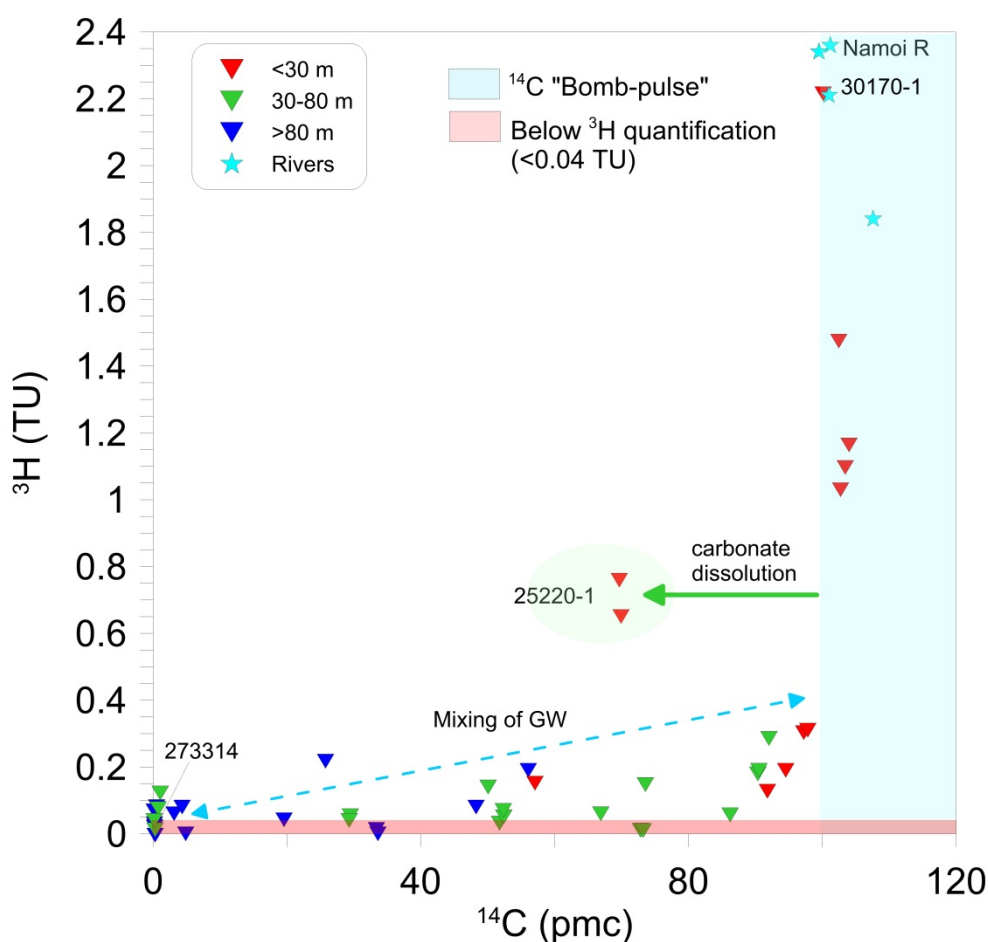513 mixing between groundwaters closer in residence times (Cartwright et al. 2013).

514

515

516 **Figure 6.** ^{3}H (TU) vs ^{14}C (pmc). This shows the mixing between groundwater with quantifiable ^{3}H

517 activity (as indicated by the red band) and groundwater with very low ^{14}C content (as indicated by the

518 dotted blue line).

519

520 **5.2   Extent of interaction between the GAB and the LNA**

521 The ^{3}H and ^{14}C values show that there is mixing between groundwater of varying residence

522 times, however they provide little constraint on the groundwaters with a ^{14}C content of close

523   to 0 pmc (ie > 30 ka). This is where chlorine-36 dating can be a useful tracer because it can

524   be used to identify the presence of groundwaters that are much older than the range provided

525   by ^{14}C.

526   A plot of ^{36}Cl/Cl vs ^{14}C (pmc) (Figure 7) shows a distinct mixing trend between

527   groundwater with high and very low ^{14}C content. The 2 deep outlying samples (30345-2 and

528   273314; shaded yellow ellipse in Figure 7) display different geochemical characteristics from

529   the other samples, possibly because of their proximity to the Napperby Formation (Figure 2).

530   Figure 7 shows the ^{36}Cl/Cl value range of GAB recharge, highlighting the alluvial samples

531   with values lower than this GAB recharge value. Calculations suggest that these particular

532   groundwater samples are potentially hundreds of thousands of years old, which is consistent

533   with groundwater from the GAB. This implies that these alluvial groundwaters are influenced

534   by artesian inflow of very old groundwater. This is evident in the natural neighbour
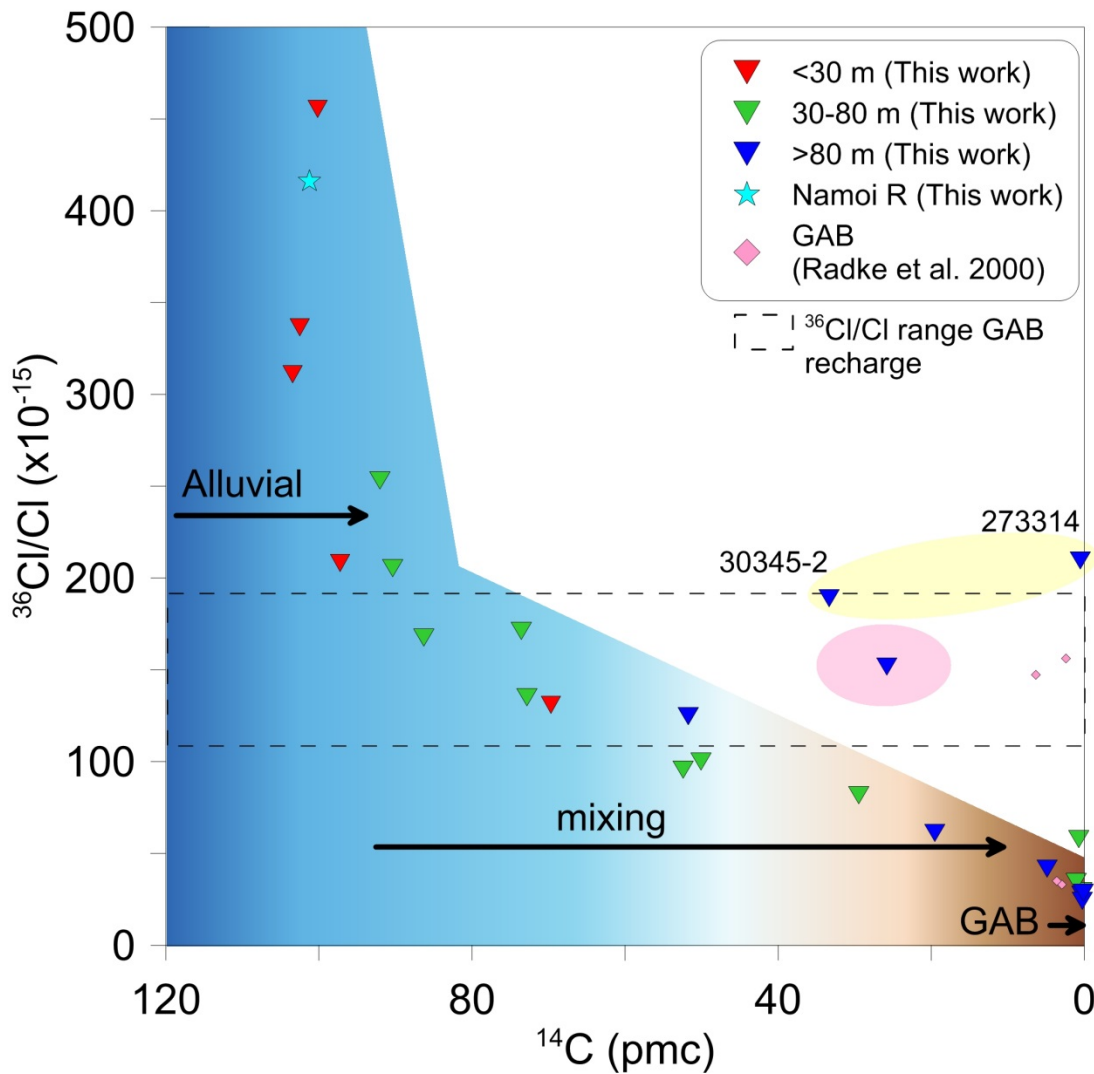
535   interpolation in Figure 2.

Figure 7. ^{36}Cl/Cl (x10^{-15}) vs ^{14}C (pmc). The colour gradient represents the mixing between the two major sources: surface water recharge (blue = modern) and the GAB (brown = old). The shaded yellow ellipse encompasses the two outliers where the geochemistry is being influenced by proximity to the Napperby Formation. The shaded pink ellipse is sample 25327-3 located in the irrigation area.

The apparent degree of ^{36}Cl decay observed in the alluvial groundwater samples is too large to be explained simply by radioactive decay as indicated by the measurable ^{14}C content in the same samples (Phillips 2000). This means that the time needed for the ^{36}Cl to decay as much as observed would be well outside the range of ^{14}C dating (> 30 ka) and therefore all groundwater samples would be expected to have a ^{14}C content of 0 pmc, which is not

547   observed. Furthermore, the decrease in ^{36}Cl is unlikely to result from dilution by ^{36}Cl-

548   depleted sources such as evaporites, as the Cl$^-$ concentrations are similar in most samples

549   (Figure 8a and b). Therefore, mixing between groundwaters of different residence times is the

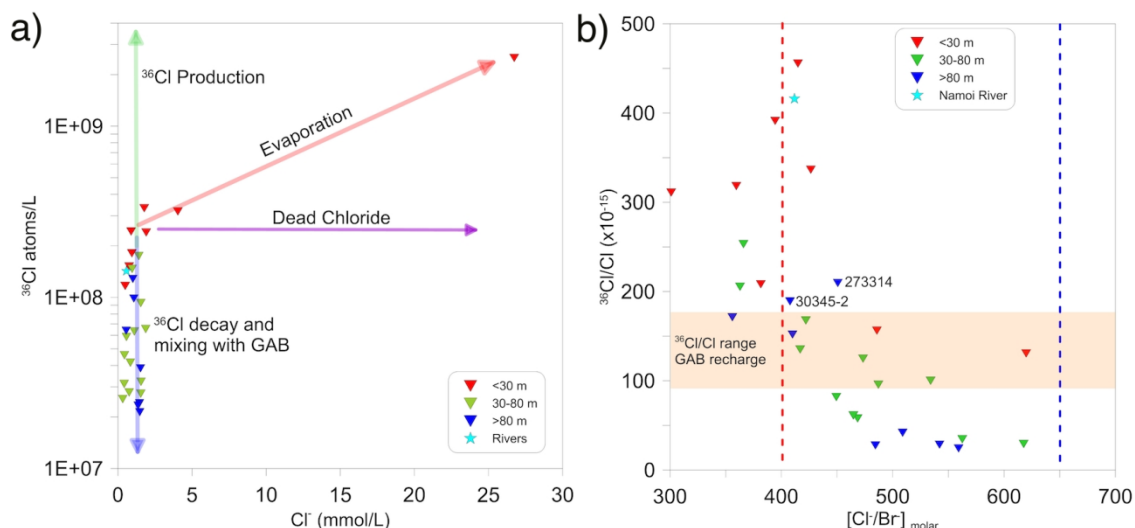550   most likely explanation for the observed ^{36}Cl signatures.

551

552   **Figure 8.** a) ^{36}Cl vs Cl$^-$ concentration. The ^{36}Cl production arrow represents potential in situ ^{36}Cl

553   production from the high U and Th content in the host rocks; b) ^{36}Cl/Cl ratio (x10^{-15}) vs Cl$^-$/Br$^-$. The

554   dotted blue line represents the Cl$^-$/Br$^-$ ratio in seawater and the dotted red line represents the expected

555   Cl$^-$/Br$^-$ ratio for rainfall at Narrabri based on distance from the coast (Short et al. 2017).

556

557   Our groundwater samples from the deep alluvium display lower ^{36}Cl/Cl ratios (down to

558   24 (x10^{-15})) than those measured in the GAB recharge zone. This indicates that there is very

559   old groundwater in the deeper LNA (conceivably older than that of the GAB recharge zone),

560   and that the mixing observed in our geochemical data could be taking place between

561   groundwater with a residence time of less than 70 years (assumed using ^{3}H) and groundwater

562   with low ^{36}Cl activities, consistent with GAB groundwater that is potentially hundreds of

563   thousands of years old (Radke et al. 2000).

564   To quantify the extent of interaction between the two groundwater sources, we use the

565   concentration of the conservative chloride ion to determine an approximate percentage of GAB

566   to alluvial groundwater at each sample location. In general, Cl concentrations in surface water

567   and shallow groundwater in the study area are low (< 30 mg/L), while samples recovered from

568   the Pilliga Sandstone (GAB) have higher concentrations (~ 60 mg/L). To estimate the local

569   surface infiltration end-member, a shallow groundwater sample with a high ^{3}H activity (sample

570   30170-1; 2.21 TU) was used. The average of all available GAB data was used for GAB inputs.

571   These end-members are mixed in varying proportions to obtain the Cl$^-$ concentration that we

572   observe in all our groundwater samples (via inverse modelling calculations). If the Cl$^-$

573   concentration in the sample was lower than that in the representative local surface infiltration

574   sample, a 100% LNA contribution is assumed. The representative sample used as the local

575   surface infiltration end-member has been subject to some evaporation and therefore does not

576   have the lowest Cl$^-$ concentration in the alluvium. If the sample with the lowest Cl$^-$

577   concentration was used as the surface water end-member, we would require a higher percentage

578   of GAB contribution across the study area. Thus, the use of the evaporated sample as our end-

579   member represents a conservative approach when considering the mixing components from

580   both the LNA and the GAB.

581   The Cl mixing results provide an approximate mixing threshold with shallower samples

582   generally containing a higher proportion of alluvial groundwater, which diminishes with

583   depth. These mixing proportions show that some deeper samples in the LNA contain up to

584   70% GAB groundwater. Figure 9 presents approximate contours for artesian discharge

585   proportions into the LNA based on the Cl mixing approach. The dotted lines indicate areas

586   where there is just one sample to inform the interpretation, whereas the solid lines connect

587   multiple samples that all displayed similar contributions from the GAB.
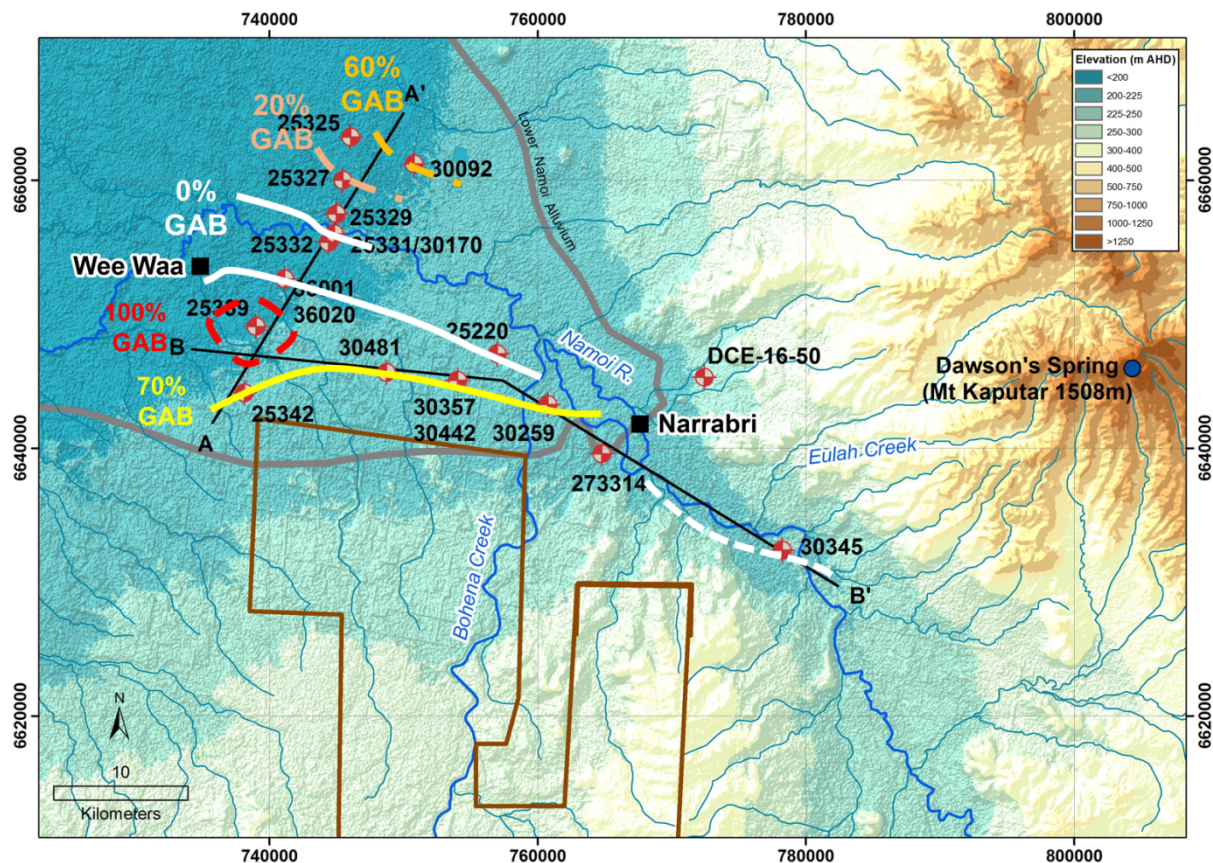
Figure 9. Approximate percentages of GAB contribution to the LNA, calculated from multiple geochemical tracers and major ion data.

Artesian input can be inferred from nested piezometers at locations 30481 and 30259 (Figure 1). At these locations, the monitoring bore slotted in the lower portion of the LNA has a head higher than the monitoring bore slotted in the shallow portion of the LNA, indicative of upward flow. At all other locations artesian contributions cannot be discerned from head data. Comparing Figure 9 to Figure 1 we show that groundwater geochemistry can provide a more accurate evaluation of GAB contribution to the LNA. This is because the geochemical data can elucidate groundwater mixing processes and provide longer term insights compared to the hydraulic head data. Multiple geochemical tracers reveal that boreholes in the north and west of the study area may be experiencing much more GAB inflow than has been inferred in catchment water balance models (Merrick 2000; Kelly et al.

602   2007; CSIRO 2007). This is most evident at sample 25342. It is not immediately apparent

603   from the vertical heads in the hydrograph set at sample 25342 that there is any GAB inflow,

604   yet based on the geochemical tracers this location is 100 % GAB groundwater. The water

605   balance model described in Merrick (2000) has GAB groundwater contributing 22% of all

606   inflow into the LNA between Narrabri and Wee Waa (Figure 1). From the geochemistry

607   alone it is not possible to make an estimate that can be directly compared to that artesian

608   discharge estimate. However, it is apparent from the mixing results shown in Figure 9 that a

609   large portion of the study area has an artesian input to the LNA that is likely to be greater

610   than 22%. The above observations highlight why geochemical insights should ideally be used

611   as one of the constraining data sets when doing water balance models in regions where there

612   is both artesian discharge and surface water recharge to the alluvial aquifer.

613

614   **5.3   Temporal changes in the interaction between the LNA and the GAB**

615   The multiple geochemical tracers we have used show substantial artesian discharge to the

616   LNA, which is larger than that currently considered in groundwater models of the region

617   (Merrick 2000; Kelly et al. 2007; CSIRO 2007). However, it is difficult to constrain how the

618   extent of artesian discharge has changed over time and how it may continue to change. Time

619   series sampling can constrain how this GAB discharge will change and is important for

620   understanding future artesian contributions to the LNA. Past ^{14}C (pmc) data collected from

621   the same bores in 1978 (Calf), 2003 (McLean), 2010 (ANSTO data) and 2016 (this study)

622   enable us to observe how the ^{14}C content in the groundwater has changed over time. The

623   historical ^{14}C data, coupled with data from this study, has the potential to be used as a

624   preliminary indicator of changes in the relative contributions of high ^{14}C contents from recent

625   surface recharge (~ 100 pmc) versus low ^{14}C contents of the GAB discharge to the LNA. The

626   dataset contains 14 bores from 5 nested sites and is the most comprehensive long-term time-

627   series database for the study area, if not Australia, despite not being complete for all years.

628   Most of the samples displayed relatively consistent ^{14}C values across the years where

629   data were available. However, we observed large changes in ^{14}C content in 5 monitoring

630   bores; 4 showed an increase and 1 showed a decrease (bold text in Table 1). This suggests

631   that the varying contributions of older and younger groundwater has changed over time,

632   which could be a preliminary indicator of increased surface recharge to various sites, or

633   increased artesian discharge to others. Therefore, measuring the ^{14}C in the groundwater at any

634   future time and assessing how this has changed using past data is useful as a preliminary

635   indicator for the current state of the system. However, consistent data collection and

636   incorporation of other factors that may affect groundwater mixing (such as rate of

637   groundwater extraction and amount of surface infiltration) are necessary to make inferences

638   about temporal changes in the interaction between the LNA and the GAB.

639

640   **Table 1.** Changes in ^{14}C content (pmc) in select boreholes in the study area between 1978-2016 (see

641   Figures 1 and 8 for the locations of the bores). The 5 bores in bold text highlight where we observe

642   changes in the ^{14}C content from 1978 to this study. Where available, the time of sampling is included.

643   ND = no data.

Bore	Depth interval (m bgs)	Calf (1978)	McLean (2003)	ANSTO data (summer 2010)	This study (summer 2016)	This study (winter 2016)
25220/1	**24.4-30.5**	**28.15**	**ND**	**ND**	**69.66**	**69.94**
25220/3	97.5-109.7	0.99	ND	0.13	0.17	0.22
25325/2	36.9-38.4	83.63	ND	85.77	86.25	ND
25325/6	**67.1-70.1**	**65.31**	**ND**	**66.57**	**90.37**	**ND**
25332/1	17.7-21	103.61	ND	ND	102.48	ND
25332/2	38.1-41.1	99.19	ND	104.78	ND	ND
25332/3	50.9-55.5	94.70	ND	ND	ND	ND
25332/4	**66.8-69.8**	**49.33**	**ND**	**84.12**	**73.57**	**ND**
25327/1	18.9-21.9	123.36	101.3 (s)	ND	103.43	102.74
25327/2	57.9-60.9	84.16	93.78 (s)	ND	92.05	90.56
25327/3	**80.8-83.8**	**8.48**	**8.63 (s)**	**ND**	**25.79**	**56.08**
30092/1	17.7-20.7	ND	90.51 (w)	ND	ND	ND
30092/2	**48.2-49.4**	**ND**	**80.06 (w)**	**72.31**	**ND**	**66.92**
30092/4	108.2-110	ND	0.19 (w)	0.24	0.3	0.21

644

6   Conclusion

646 We have used multiple geochemical tracers to show that artesian discharge to a shallow

647 alluvial aquifer is higher than previously derived from water balance models in the literature

648 (Merrick 2000; CSIRO 2007; Kelly et al. 2007). We have also provided a percentage

649 estimate of GAB groundwater in each sample collected in the LNA using the concentration

650 of Cl in the groundwater, showing that in some locations the 'alluvial' sample is comprised

651 of up to 70% GAB groundwater. Our findings are important when considering the global

652 importance of groundwater and the sustainable use of connected alluvial and artesian

653 systems, globally.

654   Isotopic tracers (^{3}H, ^{14}C, and ^{36}Cl) indicate that there is substantial mixing between two

655 groundwater end-members of very different residence times (< 70 years and very old

656 groundwater consistent with the GAB). This suggests interaction between modern surface

657 recharge through the shallow LNA and variable artesian inflow at depth, dependent on where

658 the sample is located in the system. We have also used past ^{14}C data (1978, 2003, 2010),

659 along with data from this study to show that these data can be used as a preliminary indicator

660 of how the extent of interaction between the GAB and the LNA has changed over time. Yet,

661   how these trends change geographically throughout the system, and how they will behave in

662   the future are difficult to constrain without continuous monitoring.

663   In the interval of the Lower Namoi studied discharge from the GAB into the LNA was

664   previously considered to contribute approximately less than 22% of the input water to the

665   LNA (Merrick 2000; CSIRO 2007; Kelly et al. 2007). However, the geochemical data

666   reported above clearly indicate that GAB discharge is occurring in locations where inflow is

667   not apparent from the nested hydrograph data. This highlights the need to apply multiple

668   groundwater investigation techniques (including flow modelling, hydrograph analysis,

669   geophysics, and geochemistry) when inferring artesian discharge to an alluvial aquifer. This

670   research has demonstrated that a multi-tracer geochemical approach is required to better

671   determine artesian contributions to the alluvial aquifer and must be considered in

672   constraining future models of the study system and elsewhere.

673

683

684   **Author contributions**

685 Experimental conceptualisation and design was carried out by D.I.C & B.F.J.K. Fieldwork

686 was conducted by C.P.I., D.I.C., S.I.H. & B.F.J.K. Additional data was contributed by

687 K.T.M. Geochemical analyses were conducted by C.P.I., D.I.C. & K.M.W. The manuscript

688 was written by C.P.I with input from all authors.

689

690 **Competing Interests**

691 The authors declare that they have no conflict of interest.

692

693 **6   References**

694 Abid, K., Dulinski, M., Ammar, F.H., Rozanski, K. & Zouari, K. Deciphering interaction of regional aquifers in
695 Southern Tunisia using hydrochemistry and isotopic tools. *Appl. Geochem.* **27**, 44-55, 2012.
696

697 Acworth, R.I., Timms, W.A., Kelly, B.F.J., McGeeney, D.E., Ralph, T.J., Larkin, Z.T. & Rau, G.C. Late
698 Cenozoic paleovalley fill sequence from the Southern Liverpool Plains, New South Wales – implications for
699 groundwater resource evaluation. *Aus. J. Earth. Sci.* **62(6)**, 657-680, (2015).
700

701 Airey, P.L., Calf, G.E., Campbell, B.L., Habermehl, M.A., Hartley, P.E., & Roman, D., 1979. Aspects of the
702 isotope hydrology of the Great Artesian Basin, Australia. In: Isotope Hydrology 1978, 1, P. 205–219.
703 Proceedings International Symposium on Isotope Hydrology - International Atomic Energy Agency and United
704 Nations Educational, Scientific and Cultural Organisation, Neuherberg, Fed. Rep. Germany, 19–23 June
705 1978. International Atomic Energy Agency, Vienna, 1979.
706

707 Amiri, V., Nakhaei, M., Lak, R. & Kholghi, M. Geophysical, isotopic, and hydrogeochemical tools to identify
708 potential impacts on coastal groundwater resources from Urmia hypersaline Lake, NW Iran. *Environ. Sci. Poll.*
709 *Res.* **23(16)**, 16738-16760, 2016.
710

711 Anderson, M.P. & Woessner, W.W. Applied Groundwater Modelling: Simulation of Flow and Advective
712 Transport. Academic Press. ISBN: 0-12-059485-4, 1992.
713

714 Andrews, J. N. & J.-C. Fontes, Comment on chlorine 36 dating of very old groundwater, 3, Further results on
715 the Great Artesian Basin, Australia by T. Torgersen et al., *Water Resour. Res.*, **296**, 1871–1874, 1993.
716

717 Barnett B, Townley LR, Post V, Evans RE, Hunt RJ, Peeters L, Richardson S, Werner AD, Knapton A and
718 Boronkay A. Australian groundwater modelling guidelines, Waterlines report, National Water Commission,
719 Canberra, 2012.

720

721 Barrett, C. Upper Namoi groundwater source – status report 2011. NSW Department of Primary Industries,
722 Office of Water, Sydney, 2012.

723

724 Bentley, H.W., Phillips, F.M., Davis, S.N., Habermehl, M.A., Airey, P.L., Calf, G.E., Elmore, D., Gove, H.E.
725 Torgersen, T. Chlorine 36 dating of very old groundwater. 1. The Great Artesian Basin, Australia. *Water*
726 *Resour. Res.* **22(13)**, 1986.

727

728 Beven, K. Environmental Modelling: An Uncertain Future? Routledge, ISBN-13: 978-0415457590
729 ISBN-10: 0415457599, 2009.

730

731 Calf, G.E. An investigation of recharge to the Namoi Valley aquifers using environmental isotopes. *Aust. J. Soil*
732 *Res.* **16**, 197-207, 1978.

733

734 Cartwright, I., Weaver, T., Cendón, D.I. & Swane, I. Environmental isotopes as indicators of inter-aquifer
735 mixing, Wimmera region, Murray Basin, Southeast Australia. *Chem. Geol.* **277**, 214-226, 2010.

736

737 Cartwright, I., Fifield, L.K. & Morgenstern, U. Using ^{3}H and ^{14}C to constrain the degree of closed-system
738 dissolution of calcite in groundwater. *Appl. Geochem.* **32**, 118-128, 2013.

739

740 Cendón, D.I., Larsen, J.R., Jones, B.G., Nanson, G.C., Rickleman, D., Hankin, S.I., Pyeyo, J.J. & Maroulis, J.
741 Freshwater recharge into a shallow saline groundwater system, Cooper Creek floodplain, Queensland, Australia.
742 *J. Hydrol.* **392 (3-4)**, 150-163, 2010.

743

744 Cendón, D.I., Hankin, S.I., Williams, J.P., Van der ley, M., Peterson, M., Hughes, C.E., Meredith, K., Graham,
745 I.T., Hollins, S.E., Levchenko, V. & Chisan, R. Groundwater residence time in a dissected and weathered
746 sandstone plateau: Kulnura-Mangrove Mountain aquifer, NSW, Australia. *Aus. J. Earth Sci.* **61(3)**, 475-499,
747 2014.

748

749 Chen, Z., Nie, Z., Zhang, G., Wan, L. & Shen, J. Environmental isotopic study on the recharge and residence
750 time of groundwater in the Heihe River Basin, northwestern China. *Hydrogeol. J.* **14(8)**, 1635-1651, 2006.

751

752 Clark, I.D. & Fritz, P. Age Dating Old Groundwater *in* Environmental Isotopes in Hydrogeology. CRC Press,
753 USA, 1997.

754

755 Costelloe, J.F., Irvine, E.C., Weestern, A.W. & Tyler, M. Identifying fluvial recharge and artesian upwards
756 leakage contributions to arid zone shallow, unconfined groundwater. *Chem. Geol.* **326-327**, 189-200, 2012.

757

758 CSIRO. Water availability in the Namoi. A report to the Australian Government from the CSIRO Murray-
759 Darling Basin Sustainable Yields Project. CSIRO, Australia. 154pp., 2007.

Currell, M.J., Werner, A.D., McGrath, C., Webb, J.A. & Berkman, M. Problems with the application of hydrogeological science to regulation of Australian mining projects: Carmichael Mine and Doongmabulla Springs. *J. Hydrol.* **548**, 674-682, 2017.

Dawes, W.R., Gilfedder, M., Walker, G.R. & Evans, W.R. Biophysical modelling of catchment-scale surface water and groundwater response to land-use change. *Math. Comp. Sim.* **64 (1)**, 3-12, 2004.

Department of Primary Industries (DPI) Water. NSW Government. *Namoi Alluvium Water Resource Plan (GW14), Status and Issues Paper*, available at: http://www.water.nsw.gov.au/__data/assets/pdf_file/0020/701732/Status-and-Issues-Paper-Namoi-GW-WRP.pdf, 2017.

Duvert, C., Stewart, M.K., Cendón, D.I. and Raiber, M. Time series of tritium, stable isotopes and chloride reveal short-term variations in groundwater contribution to a stream. *Hydrol. Earth Syst. Sci.* **20**, 257-277, 2016.

Edmunds, W.M. Geochemistry's vital contribution to solving water resource problems. *Appl. Geochem.* **24**, 1058-1073, 2009.

Fink, D., Hotchkis, M., Hua, Q., Jacobsen, G., Smith, A.M., Zoppi, U., Child, D., Mifsud, C., van der Gaast, H., Williams, A. & Williams, M. The ANTARES AMS facility at ANSTO. *Nuc. Instr. Meth. Phys. Res. Sect. B: Beam Interac. Mat. Atoms* **223-224**, 109-115, 2004.

Gardner, W.P., Harrington, G.A. & Smerdon, B.D. Using excess ^{4}He to quantify variability in aquitard leakage. *J. Hydrol.* **468-469**, 63-75, 2012.

Giambastiani, B.M.S., McCallum, A.M., Andersen, M.S., Kelly, B.F.J. & Acworth, R.I. Understanding groundwater processes by representing aquifer heterogeneity in the Maules Creek Catchment, Namoi Valley (New South Wales, Australia), *Hydrogeol. J.* **20(6)**, 1027-1044, 2012.

Golder Associates Santos Gunnedah Basin CSG Project. Groundwater impact study – Kahlua pilot test. Report No. 107626100-005-Rev1. Golder Associates, Australia. 2010.

Herczeg, A.L., Torgersen, T., Chivas, A.R. & Havermehl, M.A. Geochemistry of ground waters from the Great Artesian Basin, Australia. *J. Hydrol.* **126**, 225-245, 1991.

Hocking, M. & Kelly, B.F.J. Groundwater recharge and time lag measurement through Vertosols using impulse response functions. *J. Hydrol.* **535**, 22-35, 2016.

799 Iverach, C.P., Cendón, D.I., Hankin, S.I., Lowry, D., Fisher, R.E., France, J.L., Baker, A. & Kelly, B.F.J.
800 Assessing connectivity between an overlying aquifer and a coals seam gas resource using methane isotopes,
801 dissolved organic carbon and tritium. *Sci. Rep*. **5**, 1-11, 2015.

803 Jasechko, S. Partitioning young and old groundwater with geochemical tracers. *Chem. Geol.* **427**, 35-42, 2016.

805 Kalaitzis, P. & Jamieson, M. Draft Status Report for the Alluvial Groundwater Resources of the Lower Namoi
806 Valley NSW. Land and Water Conservation Groundwater Unit Barwon Region, 121pp., 2000.

808 Kelly, B.F.J., Merrick, N., Dent, B., Milne-Home, W. & Yates, D. Groundwater Knowledge and Gaps in the
809 Namoi Catchment Management Area. Cotton Catchment Communities CRC, University of Technology, Sydney
810 – National Centre for Groundwater Management Report, NCGM 2007/1, 70pp., 2007.

812 Kelly, B.F.J., Timms, W.A., Andersen, M.S., McCallum, A.M., Blakers, R.S., Smith, R., Rau, G.C., Badenhop,
813 A., Ludowici, K. & Acworth, R.I. Aquifer heterogeneity and response time: the challenge for groundwater
814 management. *Crop & Past. Sci.* **64**, 1141-1154, 2013.

816 Kelly, B.F.J., Timms, W., Ralph, T.J., Giambastiani, B.M.S., Communian, A., McCallum, A.M., Andersen,
817 M.S., Blakers, R.S., Acworth, R.I. & Baker, A. A reassessment of the Lower Namoi Catchment aquifer
818 architecture and hydraulic connectivity with reference to climate drivers. *Aus. J. Earth Sci.* **61**, 501-511, 2014.

820 Lower Namoi Groundwater, NSW Government Department of Water and Energy, DWE_08_011, 2008,
821 http://www.water.nsw.gov.au/__data/assets/pdf_file/0005/548699/wsp_namoi_gw_info_sheet.pdf

823 Love, A.J., Herczeg, A.L., Sampson, L., Cresswell, R.G., & Fifield, L.K. Sources of chloride and implications
824 for 36Cl dating of old groundwater, southwestern Great Artesian Basin, Australia, *Water Resour. Res.* **36**, 1561-
825 1574, 2000.

827 Mahara, Y., Habermehl, M.A., Miyakawa, K., Shimada, J. and Mizuochi, Y. Can the 4He clock be calibrated by
828 36Cl for groundwater dating? Nucl. Instr. Meth. in Phys. Res. Sect. B: Beam Interactions with Materials and
829 Atoms **259**, 536-546, 2007.

831 Mahara, Y., Habermahl, M.A., Hasegawa, T., Nakata, K., Ransley, T.R., Hatano, T., Mizuochi, Y., Kobayashi,
832 H., Nimomiya, A., Senior, B.R., Yasuda, H. & Obta, T. Groundwater dating by estimation of groundwater flow
833 velocity and dissolved 4He accumulation rate calibrated by 36Cl in the Great Artesian Basin, Australia. *Earth
834 Planet. Sci. Lett.* **287**, 43-56, 2009.

836 Martin, H.A. Cenozoic climatic change and the development of the arid vegetation in Australia. *J. Arid Environ.*
837 **66(3)**, 533-563, 2006.

839   Martinez, J.L., Raiber, M. & Cendón, D.I. Using 3D geological modelling and geochemical mixing models to
840   characterise alluvial aquifer recharge sources in the upper Condamine River catchment, Queensland, Australia.
841   *Sci. Tot. Environ.* **574**, 1-18, 2017.

842

843   Mawhinney, W. *Namoi Water Quality Project 2002-2007 – Final report*, NSW Office of Water, Sydney, 39 pp,
844   2011. Available at: http://pandora.nla.gov.au/pan/126486/20110413-1101/namoiwater.pdf

845

846   McLean, W.A. *Hydrogeochemical evolution and variability in a stressed alluvial aquifer system: Lower Namoi*
847   *River catchment, NSW*. PhD thesis, University of New South Wales, Sydney (unpublished), 2003.

848

849   Meredith, K.T., Han, L.F., Hollins, S.E. Cendón, D.I., Jacobsen, G.E. & Baker, A. Evolution of chemical and
850   isotopic composition of inorganic carbon in a complex semi-arid zone environment Consequences for
851   groundwater dating using radiocarbon. *Geochim. et Cosmochim. Acta* **188**, 352-367, 2016.

852   Merrick, N.P. *Optimisation Techniques for Groundwater Management*. PhD Thesis, University of Technology,
853   Sydney (unpublished), 551p.

854

855   Mook & van der Plicht. Reporting 14C activities and concentrations. *Radiocarbon* **41**, 227-239, 1999.

856

857   Moya, C.E., Raiber, M., Taulis, M. and Cox, M.E. Using environmental isotopes and dissolved methane
858   concentrations to constrain hydrochemical processes and inter-aquifer mixing in the Galilee and Eromanga
859   Basins, Great Artesian Basin, Australia. *J. Hydrol.* **539**, 304-318, 2016.

860

861   Nishiizumi, K. 10Be,26Al,36Cl, and 41Ca AMS standards: Abstract O16-1. In 9th Conference on Accelerator
862   Mass Spectrometry, page 130, 2002.

863

864   NSW   Pinneena   Groundwater   Database,   NSW   Government   DPI   Water,   available   at:
865   http://allwaterdata.water.nsw.gov.au/water.stm, (last access: 19 May 2017), 2017.

866

867   Phillips, F.M. Chlorine-36, *in* Environmental Tracers in Subsurface Hydrology. Pp 299-348, 2000

868

869   Plummer & Glynn. Radiocarbon dating in groundwater systems.   In: Isotope methods for dating old
870   groundwater: — Vienna : International Atomic Energy Agency, 2013. Pp. 33-89, STI/PUB/1587, 2013.

871

872   Powell, J. & Scott, F. A representative irrigation farming system in the Lower Namoi Valley of NSW: an
873   economic analysis. Economic Research Report No. 46, Industry and Investment NSW, 63pp., 2011.

874

875   Price, G. & Bellis, L. Namoi Catchment Water Study Independent Report Final Study Report. Schlumberger
876   Water Services (Australia) Pty Ltd, 50371/P4-R2 FINAL, 129pp., 2012.

877

878   Puls, R.W. & Barcelona, M.J. Low-flow (minimal drawdown) groundwater sampling procedures. EPA/540/S-
879   95/504, 10pp., 1996.
880

881   Radke, B.M., Ferguson, J., Cresswell, R.G., Ransley, T.R. & Habermehl, M.A. Hydrochemistry ad implied
882   hydrodynamics of the Cadna-owie-Hooray Aquifer Great Artesian Basin. *Bureau of Rural Sciences, Canberra,*
883   2000.
884

885   Raiber, M., Webb, J.A., Cendón, D.I., White, P.A. & Jacobsen, G.E. Environmental isotopes meet 3D
886   geological modelling: Conceptualising recharge and structurally-controlled aquifer connectivity in the basalt
887   plains of south-western Victoria, Australia. *J. Hydrol.* **527**, 262-280, 2015.
888

889   Rawling, G.C. & Newton, B.T. Quantity and location of groundwater recharge in the Sacramento Mountains,
890   south-central New Mexico (USA), and their relation to the adjacent Roswell Artesian Basin. *Hydrogeol. J.*
891   **24(4)**, 757-786, 2016.
892

893   Reilly T.E. and Harbaugh A.W. Guidelines for Evaluating Ground-Water Flow Models, USGS Scientific
894   Investigations Report 2004-5038, available at: https://pubs.usgs.gov/sir/2004/5038/PDF.htm, 2004.
895

896   Robertson, W.D. & Cherry, J.A. Tritium as an indicator of recharge and dispersion in a groundwater system in
897   Central Ontario. *Water Resour. Res.* **25(6)**, 1097-1109, 1989.
898

899   "Drilling Methods Bring Spectacular Yield Increases." Rural Forum for Applied Research *in* North Western
900   Courier [Narrabri] 11 Dec. 1967: 2. Print.
901

902   Salameh, E. & Tarawneh, A. Assessing the imapcts of uncontrolled artesian flows on the management of
903   groundwater resources in the Jordan Valley. *Environ. Earth Sci.* **76**, 2017.
904

905   Scanlon, B.R., Healy, R.W. & Cook, P.G. Choosing appropriate techniques for quantifying groundwater
906   recharge. *Hydrogeol. J.* **10 (1)**, 18-39, 2002.
907

908   Schilling, K.E., Jacobsen, P.J., Libra, R.D., Gannon, J.M., Langel, R.J. & Peate, D.W. Estimating groundwater
909   age in the Cambrian-Ordovician aquifer in Iowa: implications for biofuel production and other water uses.
910   *Environ. Earth Sci.* **76(2)**, 2016.
911

912   Sharma, P., Kuhik, P.W., Fehn, U., Gove, H.E., Nishiizumi, K. & Elmore, D. *Nucl. Instr. Meth. B.* **52**, 410-415,
913   1990.
914

915   Short, M.A., de Caritat, P. & McPhail, D.C. Continental-scale variation in chloride/bromide ratios of wet
916   deposition. *Sci. Tot. Environ.* 574, 1533-1543, 2017.
917

918 Stone, J.O., Allan, G.L., Fifield, L.K., et al. Cosmogenic chlorine-36 from calcium spallation. *Geochim. et*
919 *Cosmochim. Acta* **60**:679–692, 1996.

920

921 Smithson, A.*Lower Namoi Groundwater Source: Groundwater Management Area 001 Groundwater Status*
922 *Report 2008*, NSW Department of Water and Energy, Sydney, 2009.

923

924 Tadros, N.Z. The Gunnedah Basin, New South Wales. Vol. 12. *Department of Mineral Resources, Coal and*
925 *Petroleum Geology Branch*, 1993.

926

927 Tadros, C.V., Hughes, C.E., Crawford, J., Hollins, S.E. & Chisari, R. Tritium in Australian precipitation: A 50
928 year record. *J. of Hydrol.* **513**, 262-273, 2014.

929

930 Torgersen, T., Habermehl, M.A., Phillips, F.M., Elmore, D., Kubik, P., Jones, G.B., Hemmick, T. & Gove, H.E.
931 Chlorine 36 Dating of Very Old Groundwater: 3. Further studies in the Great Artesian Basin, Australia. *Water*
932 *Resour. Res.* **27(12)**, 3201-3213, 1991.

933

934 Tosaki, Y., Tase, N., Massmann, G., Nagashima, Y., eki, R., Takahashi, T., Sasa, K., Sueki, K., Matsuhiro, T.,
935 Miura, T. & Bessho, K. Application of ^{36}Cl as a dating tool for modern groundwater. *Nuc. Instr. Methods in*
936 *Phys. Res. Sect. B: Beam Interact. with Mat. and Atoms.* **259(1)**, 479-485, 2007.

937

938 Wilcken, K.M., Fink, D., Hotchkis, M.A.C., Garton, D., Button, D., Mann, M., Kitchen, R., Hauser, T. &
939 O'Connor, A. Accelerator Mass Spectrometry on SIRIUS: New 6 MV spectrometer at ANSTO, *Nucl. Inst. &*
940 *Meth. in Phys. Res. B* xxx, xxx-xxx http://dx.doi.org/10.1016/j.nimb.2017.01.003, 2017.

941 Williams, R.M., Merrick, N.P. & Ross, J.B. Natural and induced recharge in the Lower Namoi Valley, New
942 South Wales *in* Sharma, M.L. (ed.) *Groundwater Recharge,* Proceedings of the Symposium on Groundwater
943 Recharge, 239-253, 1989.

944 Zhang, L., Walker, G.R. & Dawes, W.R. Water balance modelling: concepts and applications. In. *Regional*
945 *Water and Soil Assessment for Managing Sustainable Agriculture in China and Australia.* ACIAR Monograph
946 No. 84, 31-47, 2002.

947

948 **List of Figures**

949 **Figure 1.** Map of the study area and sample locations, along with the location of the study

950 area in Australia. Accompanying hydrographs show the groundwater level response in

951 different piezometers throughout the study area (groundwater level data sourced from BOM

952 2017). The different colours in the hydrographs represent the different monitoring bores in

953 the nested set. The bottom of the slotted interval for each bore is shown in the key. The x-axis

954 in each hydrograph is the year (1970-2010) and the y-axis is depth (between 0 and 40 m

955 below ground surface (bgs)). The two locations with red text highlight areas where the

956 hydrograph heads show clear GAB contribution, with the deeper piezometer showing a

957 higher head than the shallow one. The remaining locations show no apparent GAB

958 contribution to the LNA based on the hydrograph data.

959 **Figure 2.** A geological map of the study area and two cross sections through the study area,

960 showing the location and depth of the samples in the alluvium and their proximity to

961 formations of the GAB. Contacts obtained from gas wells Nyora-1, Culgoora-1 and

962 Turrawan-2, coinciding with our cross sections, are added. Their locations are displayed on

963 the map. The general direction of groundwater flow is from SE-NW, aligning with the B-B'

964 line on the map. The chlorine-36 data interpolated using the 'natural neighbours' algorithm is

965 shown in each cross section.

966 **Figure 3.** a) Na^+ vs HCO_3^- showing the mixing trend that the alluvial samples form between

967 the Namoi River and samples from the GAB (Radke et al. 2000; McLean 2003). The orange

968 calcite saturation line indicates samples that are more enriched due to separate

969 evapotranspiration and calcite precipitation. The shaded blue ellipse represents all river

970 chemistry data available for the Namoi River and tributaries (this work (n=4), McLean 2003

971 (n=4), Mawhinney 2011 (n=79)); b) Na^+ vs F^- and c) Cl^-/Br^- vs Cl^-, highlighting the mixing

972 trend between the surface recharge and the GAB that we observe in other geochemical

973 indicators. The red dotted line represents the Cl^-/Br^- ratio for rainfall and the blue dotted line

974 is the seawater ratio.

975 **Figure 4.** Water stable isotopes in the LNA, showing the two separate mechanisms of

976 recharge; surface water recharge plotting along an evaporation trend line and potential inflow

977 from the GAB clustered with regional samples from the GAB (McLean 2003).

978   **Figure 5.** Plot of depth vs ^{3}H, highlighting the ^{3}H activity throughout the vertical

979   groundwater profile. Samples that fall within the pink zone on the left are below the

980   quantification limit (< 0.04 TU). These data are not included in our interpretation of how ^{3}H

981   changes with depth. They are presented to convey the relative proportions of interpretable

982   versus non-interpretable data.

983   **Figure 6.** ^{3}H (TU) vs ^{14}C (pmc). This shows the mixing between groundwater with

984   quantifiable ^{3}H activity (as indicated by the red band) and groundwater with very low ^{14}C

985   content (as indicated by the dotted blue line).

986   **Figure 7.** ^{36}Cl/Cl (x10^{-15}) vs ^{14}C (pmc). The colour gradient represents the mixing between

987   the two major sources: surface water recharge (blue = modern) and the GAB (brown = old).

988   The shaded yellow ellipse encompasses the two outliers where the geochemistry is being

989   influenced by proximity to the Napperby Formation. The shaded pink ellipse is sample

990   25327-3 located in the irrigation area.

991   **Figure 8.** a) ^{36}Cl vs Cl^{-} concentration. The ^{36}Cl production arrow represents potential in situ

992   ^{36}Cl production from the high U and Th content in the host rocks; b) ^{36}Cl/Cl ratio (x10^{-15}) vs

993   Cl^{-}/Br^{-}. The dotted blue line represents the Cl^{-}/Br^{-} ratio in seawater and the dotted red line

994   represents the expected Cl^{-}/Br^{-} ratio for rainfall at Narrabri based on distance from the coast

995   (Short et al. 2017).

996   **Figure 9.** Approximate percentages of GAB contribution to the LNA, calculated from

997   multiple geochemical tracers and major ion data.

998